Methane Emissions to the Atmosphere from the Scotia and Weddell Seas

Evelyn Workman[1,2], Anna E. Jones[1], Rebecca E. Fisher[2], James L. France[2,3], Katrin Linse[1], Bruno Delille[4], Freya A. Squires[1]

[1]British Antarctic Survey, Natural Environment Research Council, Cambridge, CB3 0ET, UK
[2]Centre of Climate, Oceans and Atmosphere (COCOA), Department of Earth Sciences, Royal Holloway University of London, Egham, TW20 0EX, UK
[3]Environmental Defense Fund, London, EC3M 1DT, UK
[4]Chemical Oceanography Unit, Freshwater and Oceanic sCience Unit reSearch (FOCUS), University of Liège, Liège, Belgium

Key Points:

- This study combines seafloor activity, and water column and atmospheric methane observations in the Weddell and Scotia seas, Southern Ocean.
- The entire study area was found to be a source of atmospheric methane, contrasting to previous studies.
- CH_4 emissions vary by latitude and depth, with less emitted south of the Southern ACC front and higher emissions from on-shelf regions.

Corresponding author: Evelyn Workman, eveman85@bas.ac.uk

Abstract

The Southern Ocean's role in the global methane (CH_4) cycle remains uncertain due to limited measurement data from this remote region. It is unclear if the Southern Ocean acts as a source or sink of atmospheric CH_4, and climatic changes can have consequences on the amount of marine CH_4 released due to the acceleration of glacial melting and uncertain consequences on seabed CH_4 reservoirs. Monitoring CCH_4H4 here is essential to understanding its impact on the global CH_4 budget now and in the future. This study measured CH_4 concentrations in both ocean and atmosphere during an expedition in the Scotia Sea, Weddell Sea, and South Georgia shelf, linking seabed activity, water column concentrations, sea-air fluxes, and atmospheric CH_4 levels. All areas were found to be a small source of CH_4 to the atmosphere. Surface water CH_4 concentrations varied latitudinally, with lower CH_4 levels south of the Southern Antarctic Circumpolar Current front, where upwelling brings CH_4-depleted waters to the surface. On-shelf regions show higher CH_4 emissions compared to off-shelf, with average sea-air CH_4 fluxes of 0.269 ± 0.035 µmol m^{-2} d^{-1}and 0.136 ± 0.021 µmol m^{-2} d^{-1}, respectively, likely due to seabed seepage and methane-enriched freshwater. This study finds that the Weddell and Scotia seas (including the South Georgia shelf) are a small source of atmospheric CH_4. As this result contradicts previous studies identifying this region as a CH_4 sink, continued monitoring is needed to understand how emissions are changing and may continue to change in the future.

Plain Language Summary

Methane is a powerful greenhouse gas. The amount of methane released from the Southern Ocean into the atmosphere remains unclear, but it is important to better understand the Southern Ocean's role in the global methane budget and how this may change in the future under future climate change scenarios. This study investigates methane concentrations in the ocean and the atmosphere during an expedition on RRS Discovery in the South Atlantic and Southern Ocean in December 2022 and January 2023 to attempt to understand the impact this region has on atmospheric methane concentrations. This study finds that this region is a small source of atmospheric methane. This changes our understanding of this region in the global methane cycle, as previous studies have found the region to be a sink of methane. On-shelf regions (South Georgia shelf) emit more methane per area than off-shelf regions due to local methane sources such as methane seeping from the seabed and methane-enriched freshwater outflowing from land. Deeper water masses in the Scotia and Weddell seas (Antarctic Bottom Water) contain less methane than the shallower waters (Antarctic Surface Water). It is important to understand if methane dynamics in this region will continue changing and their impact on atmospheric emissions. Continued monitoring of methane in water, air, and sea-air fluxes is necessary.

1 Introduction

Methane (CH_4) is a potent greenhouse gas, which has a global warming potential greater than CO_2, with a radiative forcing 80 to 83 times that of CO_2 over a 20 year period (Forster et al., 2021). Atmospheric CH_4 has natural and anthropogenic sources and concentrations have been increasing since the beginning of the industrial revolution (Saunois et al., 2024). In general, the global ocean is understood to be a small source of atmospheric CH_4, constituting 1-3 % of the global methane budget (Saunois et al., 2024), however the amount of CH_4 released is not well constrained. In particular, the role the Southern Ocean plays in the global CH_4 cycle is unclear, as previous studies have identified certain regions as sources (Yoshida et al., 2011; Bui et al., 2018; Polonik et al., 2021; Workman, Fisher, et al., 2024) and others as sinks (Heeschen et al., 2004; Ye et al., 2023; Workman, Fisher, et al., 2024) during summertime months, highlighting significant regional variability and uncertainty. Data in this region are limited due to the remoteness of the area, however it is important that this component is better constrained to understand the impact on global CH_4 concentrations and to monitor how this may be changing.

There are several sources of CH_4 in the Southern Ocean. CH_4 can be produced in the seabeds around the Antarctic/sub-Antarctic as these provide the anoxic environment for CH_4 to be produced biogenically from CO_2 by methanogenic archaea (Reeburgh, 1980; Whiticar, 1999; Hinrichs & Boetius, 2002; Formolo, 2010). This biogenically produced CH_4 can either be modern (from recent microbial activity) or geological (from ancient fossil microbial activity) (Saunois et al., 2024). Methane in sediments can also be produced thermogenically, by thermal breakdown of organic matter over geological timescales in the Earth's crust (Saunois et al., 2024). Some of this sedimentary CH_4 (modern or geological) can be stored in CH_4 hydrates in the seabed of continental shelves and slopes. Hydrates are ice-like structures consisting of CH_4 and water, stable only under certain low temperature and high pressure conditions (Milkov, 2005), within the gas hydrate stability zone (GHSZ). If hydrates become unstable (e.g. due to rising temperatures or decreasing pressures) they can dissociate and release CH_4 into the water column (Ruppel, 2011). The remaining CH_4 not stored in hydrates is mostly broken down via anaerobic oxidation of CH_4 within the sediments. However, a small fraction can be transferred into the water column by diffusion or in bubbles (ebullition) from gas seeps. Most gas bubbles will dissolve as they rise up the water column, with the CH_4 being oxidised by aerobic methane oxidising bacteria (methanotrophs) in the water, which can leave only a small fraction of the initial CH_4 reaching the surface waters. More CH_4 can reach the surface if a substantial amount is released from the seabed and the waters are sufficiently shallow to limit the impact of microbial oxidation (McGinnis et al., 2006; Ruppel & Kessler, 2017).

CH_4 seepage from the seabed in the Arctic Ocean has been observed in a greater number of studies than in the Southern Ocean. For example, off the west coast of Svalbard numerous studies have identified seeps and gas flares (Knies et al., 2004; Westbrook et al., 2009; Rajan et al., 2012; Sahling et al., 2014; Graves et al., 2015; Steinle et al., 2015; Mau et al., 2017; Veloso et al., 2019; Dølven et al., 2022), which have been linked to the degradation of CH_4 hydrates at the West Svalbard continental margin. Westbrook et al. (2009) and Berndt et al. (2014) have attributed this hydrate breakdown to warming Atlantic bottom waters that flow northwards as the West Spitzbergen Current to this area. By comparison, CH_4 flares from gas seeps have been identified in several places around the Antarctic/sub-Antarctic using ship-borne acoustic data. Numerous flares have been found emanating from the continental shelf around the island of South Georgia (Römer et al., 2014; Geprägs et al., 2016; Bohrmann et al., 2017; Workman, Fisher, et al., 2024). This sedimentary CH_4 has been found to be of microbial origin, by isotopic analysis of sedimentary gas (Römer et al., 2014; Geprägs et al., 2016). However, there is limited knowledge on how much of this CH_4 makes it into the atmosphere. Seabed seeps have also been observed via gas flare detection around the Antarctic Peninsula, including around King George Island (Workman, Fisher, et al., 2024), Deception Island (Workman, Fisher, et al., 2024), Seymour Island (del Valle et al., 2017), and the Kerguelen Plateau (Spain et al., 2020), via in-situ imagery in the Ross Sea by Thurber et al. (2020) and Seabrook et al. (2023), and inferred from CH_4 measurement in the Bransfield Strait (Polonik et al., 2021).

In addition to CH_4 being produced in anoxic seabed sediments, methanogenesis (production of methane) is also thought to occur in the oxygen-rich upper waters of the ocean (Karl et al., 2008). CH_4 production by phytoplankton is a potential pathway that can explain this so-called 'ocean methane paradox' (Lenhart et al., 2016; Klintzsch et al., 2019, 2020; Bižić et al., 2020; Bižić, 2021). This is the paradox of CH_4 production in oxygen-rich surface waters, even though oxygen typically hinders methane production. CH_4 has also been shown to be produced in oxic upper waters from demethylation of substances such as organic phosphonates (Repeta et al., 2016), methylamines (Bižić-Ionescu et al., 2018) and DMSP (dimethylsulfoniopropionate) (Damm et al., 2010). Plastic has been proposed as an additional potential pathway for CH_4 production in oxygen-rich water, for example, Royer et al. (2018) found that plastic can produce and release CH_4 abiotically when exposed to solar radiation. However, in the Southern Ocean, there is a lower density of plastics (micro- and macro-) compared to other oceans (Suaria et al., 2020), meaning that the impact of plastics on CH_4 production in the Southern Ocean is probably less than in other oceans.

Outflow of glacial water from land can be a source of CH_4 to coastal oceans in Antarctic/sub-Antarctic regions. CH_4 can be produced in subglacial sediments by methanogens, leading to subglacial meltwater which is supersaturated in CH_4 (Christiansen & Jørgensen, 2018; Burns et al., 2018; Lamarche-Gagnon et al., 2019), which can be carried into the ocean in glacial streams. This phenomenon has been identified in the West Antarctic Peninsula by Danis et al. (2024), where surface water supersaturated in CH_4 was identified in the water at the terminus of a marine terminating glacier.

The Southern Ocean has warmed due to anthropogenic climate change, which includes the warming of both surface waters and bottom waters (Antarctic Bottom Water) (Fox-Kemper et al., 2021). Warming of bottom waters in the Southern Ocean may impact the GHSZ and lead to the instability of marine gas hydrates in shelf sediments. Warmer ocean water can promote the formation of methane (CH_4) in sediments. This is primarily because higher temperatures enhance the metabolic activities of methanogenic archaea. Warmer conditions can increase the rate of organic matter decomposition, leading to more substrates available for methanogenesis. This phenomenon has already been shown for freshwater systems, e.g. Y. Zhu et al. (2023). Additionally, climate warming could exacerbate the amount of CH_4 flowing out from terrestrial sources into the ocean in the polar regions, due to increased glacial and ice sheet melt. Additionally, over much longer timescales, ice sheet loss will reduce local sea level due to isostatic rebound, and therefore reduce pressure at the seabed, causing the instability of any CH_4 hydrates around the ice sheet (Wallmann et al., 2018). Therefore, the impacts of human-caused climate warming could further exacerbate CH_4 release from the oceans around the Antarctic and sub-Antarctic, creating a positive feedback loop in climate warming.

In this study we characterise CH_4 in the South Atlantic and Southern Ocean systems using measurements of the atmospheric mixing ratio of CH_4, dissolved CH_4 concentration throughout the water column and hydroacoustic detection of CH_4 flares in the water column. As we are particularly interested in sea-air interactions to understand how the ocean surface impacts atmospheric CH_4, we calculate sea-air fluxes of CH_4. This study focuses on an on-shelf area known to be active with seabed CH_4 production and flaring in the water column, the continental shelf of South Georgia, and off-shelf area in the Scotia and Weddell seas. The aim of this study is to compare and contrast CH_4 concentrations in the deep waters, surface waters and atmosphere, and the sea-air fluxes over these different areas, in order to investigate what processes are controlling CH_4 in the water and in the atmosphere.

2 Materials and Methods

2.1 Study area

Data collection and air measurements for this study were conducted over approximately 9000 km during the DY158 expedition on *RRS Discovery* from Montevideo, Uruguay, departing on the 22nd December 2022 via the northern Weddell Sea to Mare Harbour, Falkland Islands, arriving 29th January 2023. The expedition traversed the South Atlantic Ocean towards the island of South Georgia, then south through the Scotia Sea and into the northern Weddell Sea, where the A23 transect (a physical oceanography transect with multiple CTD (Conductivity-Temperature-Depth) stations (Meredith et al., 2023; Zhou et al., 2023)) was carried out. The vessel then travelled west to the Orkney Passage in the Scotia-Weddell confluence, and then north through the Scotia Sea to the Falkland Islands (Figure 1).

The study region spans a large area of the South Atlantic and Southern Ocean, including several oceanographically important fronts associated with the Antarctic Circumpolar Current (ACC); Subantarctic Front (SAF), the Polar Front (PF), and the Southern ACC Front (SACCF) (Figure 1). The ACC is the dominant current in this region, and flows through the Drake Passage and east through the Scotia Sea. The study area also comprises several shelf regions including the Patagonian Shelf, the South Georgia Shelf, and the South Orkney Shelf. The continental shelf of South Georgia is an area of particular interest with respect to CH_4 as raised levels have been detected in the water column and methane bubble plumes (flares) emanating from the seabed around South Georgia have been identified in troughs and in several bays (Römer et al., 2014; Bohrmann et al., 2017). However, those studies did not observe the atmosphere, so it is unclear how much CH_4 makes it into the atmosphere. open ocean areas of the Weddell and Scotia seas lack known CH_4 sources. The water masses of these seas include Antarctic Bottom Water (AABW), Circumpolar Deep Water (CDW) and surface waters.

2.2 Atmospheric measurements

Atmospheric methane concentrations were continuously measured along the entire expedition (from Montevideo to Mare Harbour) using a Los Gatos Research (Mountain View, CA, USA) Ultra-portable Greenhouse Gas Analyzer (UGGA). The inlet of the UGGA was mounted on the meteorological mast at the front of the ship ($\sim$ 17.6 m asl (above sea level)), minimising impact of pollution from the exhaust stack at the back of the ship. A 30-metre long inlet tube with internal diameter of 3/8” (dekabon) connected the mast to the UGGA in the met lab. The UGGA took measurements of atmospheric methane, carbon dioxide and water vapour concentrations every second. A KNF pump (type N816.1.2KN.18) pulled air from the inlet down the tube. The residence time was 10 seconds. The air inlet included a funnel pointing down to minimise rain entering and a water trap (Norgren F07 series 40 µm G 1/4, part no.: F07-200-A3TG) located just downstream of the inlet, to trap the majority of the water droplets entering the inlet. There were two in line filters (7 and 2 microns) used in the setup to stop particles entering the pump/UGGA which could cause damage.

The UGGA is regularly calibrated by measuring gases of known CO_2 and CH_4 concentrations. The calibration suite consists of three 5 litre cylinders of compressed ambient air (2 calibration gases and 1 target gas, which are traceable to WMO reference scales for CH_4 and CO_2), with CO_2 and CH_4 concentrations and uncertainties as given in Table 1 of the Supporting Information (SI). The dataset is filtered based on wind direction in order to minimise contamination from pollution from the ship stack; data corresponding to wind directions between 30° and 330° relative to the ship (0° is wind coming directly from the front of the ship and 180° is wind coming directly from behind the ship) are removed. There is little variation in the data, so 2-hour averages were calculated to allow us to see any trend in the dataset.

Atmospheric CH_4 concentrations measured at Antarctic research station Neumayer III (70.67°S, 8.27°W) using a Picarro G2301 were used to detrend the ship-based measurements from seasonality. To do this the Neumayer CH_4 data were fitted with a curve using the NOAA curve fitting function (Thoning et al., 1989). This allows us to investigate the small scale variability in the atmospheric dataset without the influence of seasonal variability. We assume that the Neumayer seasonal CH_4 cycle is comparable to the seasonal cycle across the full latitudinal range of the cruise. This is justified by comparing the amplitude of the seasonal CH_4 trend of Neumayer data with CH_4 data from the

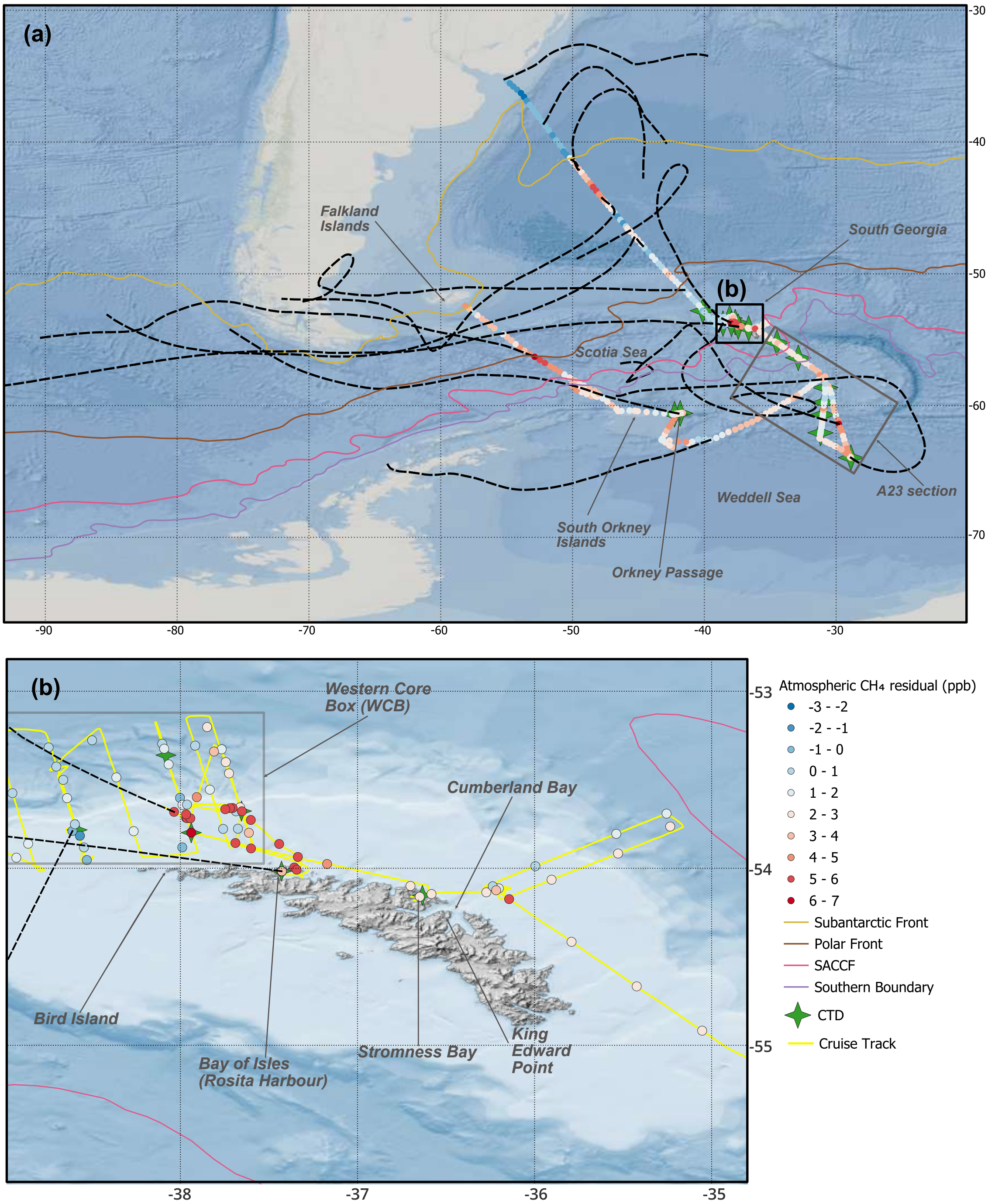

Figure 1. (a) Map of study area. 2 hour averaged atmospheric CH_4 residual concentrations (blue to red circles, with colour indicating size of residual, as defined in the legend) with 72 hours air mass back trajectories (black dashed lines) calculated using HYSPLIT model from different points along the cruise track. Residual methane concentrations are the atmospheric methane concentration measured on DY158 using UGGA, seasonally detrended using atmospheric data from research station Neumayer III, as described in Section 2.2. Oceanographic fronts: Subantarctic Front (yellow), Polar Front (brown), Southern Antarctic Circumpolar Current Front (SACCF) (pink), Southern Boundary of the Antarctic Circumpolar Current (purple). Oceanographic front positions were calculated using dataset from Park Young-Hyang (2019). The locations of CTD casts are marked with green stars. (b) Map of South Georgia with the cruise track (yellow line), locations of CTD casts (green stars), 2 hour averaged atmospheric CH_4 residual concentrations (blue to red circles). The locations of research bases Bird Island and Kind Edward Point are indicated.

NOAA Cooperative Global Air Sampling Network (Global Monitoring Laboratory, 2024) at Palmer Station (64.77°S, 64.05°W), Ushuaia (54.85°S, 68.31°W), Crozet Island (46.43°S, 51.85°E), and Cape Point (34.35°S, 18.49°E), covering the range of latitude covered during the expedition. Figure S1 in SI shows that the amplitude of the seasonal change of CH_4 is similar across the range of latitudes.

72 hour back trajectories of air masses along the cruise track were calculated using the NOAA HYSPLIT trajectory model (Stein et al., 2015) with the Global Data Assimilation System (GDAS) meteorological data at 1 degree resolution.

2.3 Water measurements

Water column samples were collected using a CTD with Niskin bottle rosette-casts and water surface samples were taken more frequently using the underway water system on the ship which has its inlet at 5 m below the sea surface. The CTD rosette contained Seabird SBE 9plus temperature and salinity sensors, AquaTracka III Fluorometer (Chelsea Technologies Group) for chlorophyll a detection and twenty-four 20 L Niskin bottles to take samples of seawater from discrete depths. The salinity measured by the Seabird SBE 9plus sensor was calibrated by sampling several Niskin bottles from each CTD cast and analysed using a Autosal salinometer. The underway water system on the ship was also calibrated using the same procedure, with samples being taken approximately every 6 hours. Temperatures measured by the CTD were calibrated using a Deep Ocean Standards Thermometer (Seabird SBE 35 DOST) which was mounted on the CTD frame.

Water samples were stored in 60 ml glass bottles. An airtight Tygon tube of the correct diameter for the 60 ml sample bottles was attached to the spout of the Niskin bottle/underway tap and the sample bottle filled. Bottles were rinsed by letting them overflow for 2-3 seconds, and filled until a meniscus formed at the top of the bottle. Each sample was then poisoned with 60 µL of saturated mercuric chloride solution (7.7 g/100 ml) to stop biological processes, which could change the methane concentration in the water before it is analysed. The bottle was then firmly closed with an isobutyl stopper, an aluminium cap was crimped on top of the stopper with a crimper wrench. The sample was stored at room temperature for the remainder of the cruise. During the transit back to the UK the samples were stored in the +4°C refrigerated storage room on *RRS Discovery*.

Water samples were analysed from 16 CTD casts (Table S2 in SI), which were chosen to cover a range of latitudes, off-shelf/on-shelf areas and in areas of particular interest due to known presence of methane seeps (South Georgia shelf). Samples were taken from full-ocean-depth CTDs, ranging from 59 m to 4890 m depth, with between 8 and 11 depth horizons for each CTD, with more samples collected near the surface, as the study focuses on dynamics at the sea-air interface. Underway water samples were taken more regularly, again at a range of latitudes and off-shelf and on shelf, usually between CTD casts. Water samples were stored for 7 to 8 months at room temperature until analysis.

Measurements of dissolved CH_4 concentration in the water samples was carried out at the University of Liège, Belgium. Samples were analysed using gas chromatography (GC) (SRI 8610 C gas chromatograph) to measure the concentration of dissolved methane concentration. The method involves creating a 20 ml headspace (using nitrogen) in the 60 ml sample bottle and allowing the water sample and the headspace to come to equilibrium by shaking for 20 minutes and leaving for $\sim$ 24 hours, then extracting the headspace air and measuring the CH_4 concentration of the headspace on the GC. The reproducibility on the measurements is 0.4 nM (standard deviation).

In this study we define surface water samples as all the underway water samples taken and all the surface samples from each CTD cast. The surface sample at each CTD location corresponds to the average CH_4 concentration of all the samples taken within the mixed layer depth (MLD) at that location. The MLD is calculated for each CTD cast and is defined as the depth at which the in-situ density exceeds 0.03 kg/m^3 plus the density at the surface (de Boyer Montégut et al., 2004).

The methane saturation of the water samples was calculated using the equation,

$$sat = C_w/C_a, \tag{1}$$

where, C_w is the dissolved CH_4 concentration in the water, C_a is the air-equilibrated seawater CH_4 concentrations (equation 2) calculated using atmospheric CH_4 mixing ratios (measured on the UGGA) averaged 1 hour rolling mean around the time the sample was taken, as well as calibrated water temperature and salinity measurements from the CTD or underway water system.

C_a is defined by Wiesenburg and Guinasso (1979) as,

$$lnC_a = lnf_G + A_1 + A_2 ln(100/T) + A_3 In(T/100) + A_4(T/100) + S‰[B_1 + B_2(T/100) + B_3(T/100)^2] \tag{2}$$

where, f_G is the mole fraction of gas in the dry atmosphere, T is the temperature in kelvin, S is the salinity in parts per thousand, A_i and B_i are constants for calculation of solubilities.

2.4 Sea-air methane flux

In this study, sea-air CH_4 flux (F) is calculated using the bulk flux equation from Wanninkhof (2014),

$$F = k(C_w - C_a) \tag{3}$$

Where, C_w is the dissolved CH_4 concentration in the water, C_a is the air-equilibrated seawater CH_4 concentrations (equation 2), as described previously. The gas transfer velocity, k, (Ho et al., 2006) is calculated,

$$k = 0.254U^2(S_c/660)^{-0.5}, \tag{4}$$

where S_c is the Schmidt number calculated following the method in Vogt et al. (2023) (equations given in Appendix A2 of Vogt et al. (2023)), where the authors use a correction for salinity based on Jähne et al. (1987) and Manning and Nicholson (2022), to calculate S_c. U is the 10 m asl wind speed. We calculate k based on the parameterisation by Ho et al. (2006), as their parameterisation was adapted for the Southern Ocean and higher wind speeds, meaning it may be more appropriate to use in this study than other parameterisations for k. ERA5 10 m wind speed reanalysis data was used to calculate k for each surface water concentration data point at every hour during the month in which the measurement occurred (December 2022 or January 2023). F was subsequently calculated for each hour for each data point and then averaged over the month for each individual data point.

2.5 Scotia Sea and Weddell Sea Water Masses

The deep-water masses present in the Weddell and Scotia seas are (from deepest to shallowest): Antarctic Bottom Water (AABW), Lower Circumpolar Deep Water (LCDW)/Warm

Deep Water (WDW), and Upper Circumpolar Deep Water (UCDW). In this study, we define the water masses based on neutral density boundaries as per Naveira Garabato et al. (2002); AABW waters have neutral densities greater than 28.26 kg/m^3, LCDW/WDW have neutral densities between 28.00 and 28.26 kg/m^3, and UCDW have densities between 27.55 and 28.00 kg/m^3. The water mass above UCDW is defined as surface water.

2.6 South Georgia methane flare investigation

Previous research, conducted by Römer et al. (2014) and Bohrmann et al. (2017), has revealed the existence of extensive methane seepage through hydroacoustic flare detection, followed by physical gas sampling and analysis, originating from the seabed surrounding South Georgia. However, the extent to which this methane actually reaches the atmosphere remains uncertain. A simplified version of the method used by Bohrmann et al. (2017) was followed to detect methane flares in the water column around South Georgia, particularly in Bay of Isles, Stromness Bay and on the northern South Georgia shelf (see Table S3 in SI). This entailed using a multibeam echosounder (*Simrad* EM710) and a single beam echosounder (*Simrad* EK80) to search for flares from the seabed. The nominal frequency of the EM710 was 100 kHz. The settings used are shown in Table S4 in SI. The EK80 on *RRS Discovery* operates at five different frequencies (18 kHz, 38 kHz, 120 kHz, 200 kHz, 333 kHz) with transducers mounted on a drop keel. The settings used by the EK80 during the methane flare survey are given in Table S5 in SI. Both EM710 and EK80 are used as the EM710 has a larger spatial range than the EK80, but flares can be seen more clearly at the lower frequencies of the EK80. Using the method described here, no flares were detected on the EM710, but flares were identified on the EK80. The EK80 data is initially viewed using the EK80 software to pinpoint exact timestamps of flares and to generate the echograms.

3 Results

3.1 Atmospheric Methane Concentrations

Atmospheric CH_4 concentrations measured in this study are compared to atmospheric CH_4 concentration measured at Antarctic research station Neumayer III (70.67°S, 8.27°W) over the same time period (Figure 2) to put the ship-based data from this study into a regional and temporal context, allowing the ship-based data to be seasonally detrended. The atmospheric CH_4 concentrations measured during the cruise have a general downward trend with time, which follows the downward seasonal trend observed in the Neumayer atmospheric CH_4 concentrations during the same time period (December 2022 and January 2023) (Figures 2a and 2b). From the HYSPLIT back trajectory analysis (Figure 1), during the first three days of the cruise the air mass originates from the Atlantic Ocean, while throughout the rest of the cruise the air masses originate mainly from the South America/Antarctica and Drake Passage. The seasonally detrended CH_4 residuals (Figure 2c) are generally elevated over the South Georgia shelf (over the approximate time period 3rd January 2023 to 6th January 2023). The back trajectories during and before the elevated period of atmospheric CH_4 concentrations on the South Georgia shelf show that the air masses originate from varying directions (Figure 1) when CH_4 is elevated.

3.2 Surface Water Methane Concentrations

The surface water dissolved CH_4 concentration measured in this study varies between 3.76 nmol/L and 29.72 nmol/L (Figure 3). The surface water CH_4 saturation (with respect to atmospheric concentration) varies between 102.1% and 844%. The surface saturation is greater than 100% for every sample across the entire study area.

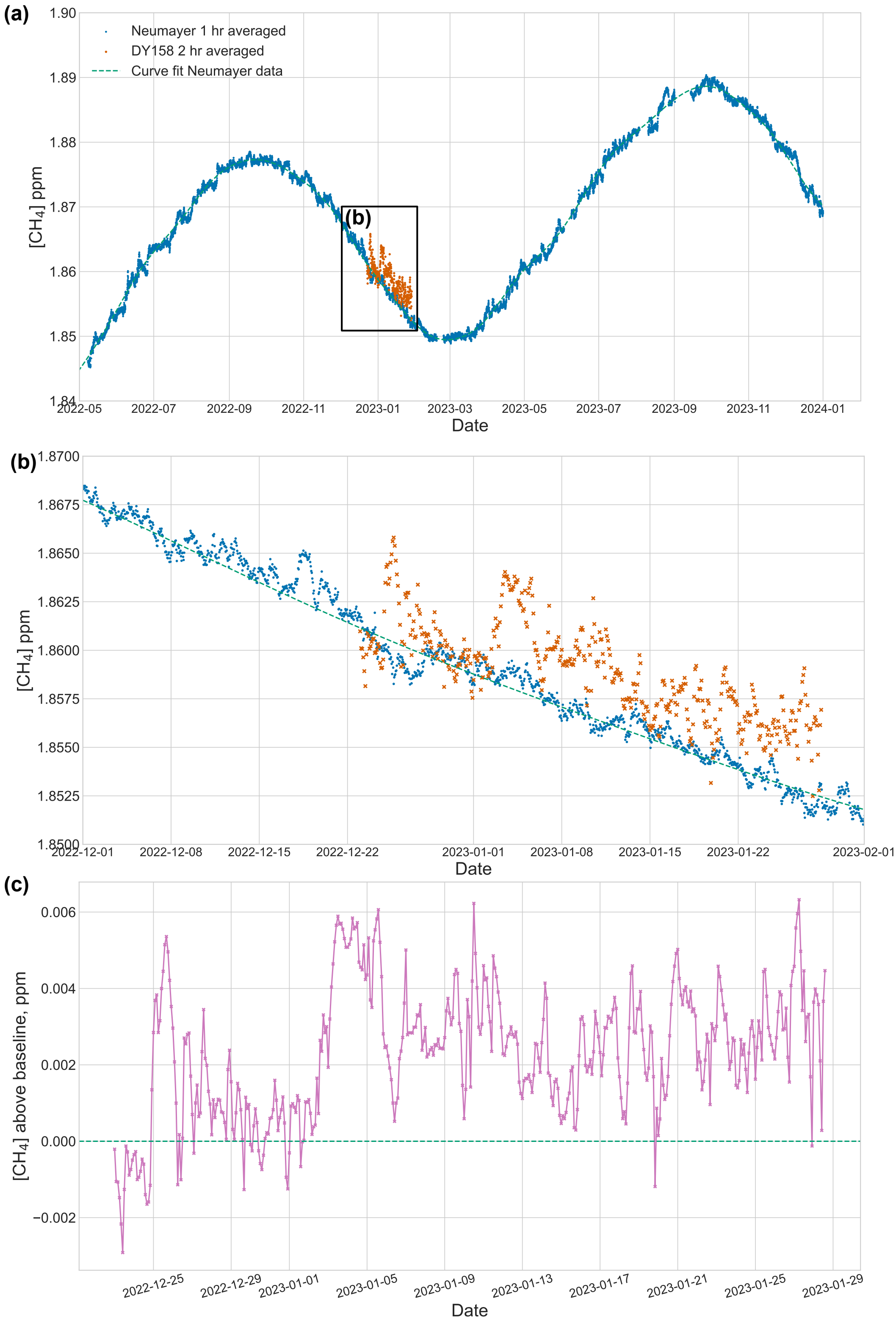

Figure 2. (a) 2 hourly averaged atmospheric CH_4 concentration measured onboard DY158 (orange) and 2 hourly averaged Neumayer data (dark blue). The curve fit of Neumayer data was calculated using NOAA's curve fitting function (Thoning et al., 1989) (teal dashed line). (b) Same as (a) but zoomed into period of DY158. (c) Atmospheric CH_4 residual (CH_4 concentration observed during DY158 minus Neumayer curve fit) (pink), zero line (teal dashed line) respresents the curve fit of the Neumayer data, as in (a) and (b).

Outlier analysis was performed on the on-shelf and off-shelf datasets independently to remove outlying data points. On-shelf refers to on the South Georgia shelf, and is defined as any data point with water depth shallower than 500 m (Heywood et al., 2014). Outliers were identified as those lying above the value derived by adding 1.5 times the interquartile range to the mean. This was calculated to be 6.74 nmol/L for the off-shelf dataset and 15.22 nmol/L for the on-shelf dataset. In carrying out this calculation, we assume that these two datasets are distinct as on-shelf and off-shelf areas have been shown to be distinct in relation to surface CH_4 concentrations in previous studies (Weber et al., 2019; Bange et al., 1994).

The mean CH_4 concentration (saturation) without outliers for all off-shelf data is 4.92 ± 0.14 nmol/L (144% ± 5%) and for all on-shelf data is 6.37 ± 0.62 nmol/L (188% ± 18%), implying that surface concentrations are greater on-shelf than off-shelf. The mean surface water CH_4 concentration (without outliers) is 5.18 ± 0.21 nmol/L north of the Southern Antarctic Circumpolar current front (SACCF), and 4.73 ± 0.19 nmol/L south of the SACCF, indicating lower surface water CH_4 concentration south of the SACCF. Errors quoted are standard errors of the mean.

3.3 Water Column Methane Concentrations

3.3.1 Scotia Sea and Weddell Sea

Water column profiles from CTD casts reveal that surface waters in the open ocean of the Weddell and Scotia seas are consistently more enriched in dissolved CH_4 compared to deeper waters (Figure 4). Sampling sites included one cast within the Antarctic Circumpolar Current, four within the Weddell Scotia Confluence, and four in the Weddell Gyre (Figure 4a). The surface layers were at or above saturation compared to the atmosphere, however deeper waters were undersaturated. Most water profiles have an increase in CH_4 concentration/saturation at ∼ 100 m. For some profiles this increase corresponds with an increase in chlorophyll a concentration (i.e. Figures 4b and 4e). However, this is not universally the case across all the water profiles, e.g. in Figure 4d the chlorophyll a peak occurs at a shallower depth (∼ 50 m), while the CH_4 peak is at ∼ 100 m. Typically, at water depths of greater than 100 m, the waters become undersaturated in CH_4 (Figure 4).

For Scotia and Weddell sea water masses, we calculated the average concentration of CH_4 to be 1.93 ± 0.08 nmol/L in AABW, 2.44 ± 0.13 nmol/L in LCDW, and 4.34 ± 0.73 nmol/L in UCDW, showing a clear gradient where deeper water masses have lower CH_4 concentrations than the shallower ones. This depletion of CH_4 in deeper waters reflects the relative enrichment of methane in the upper water masses (Figure 5). The errors quoted are standard error of the mean.

3.3.2 South Georgia

There were 6 CTD casts deployed around South Georgia to collect water samples for dissolved CH_4 concentrations (Figure 6). 5 of these were on the South Georgia shelf (310 m to 59 m water depth) and 1 was off-shelf in 2666 m water depth. We split South Georgia water column profiles into three regimes; off-shelf (CTD WCB 3.2N (Figure 6g)), on-shelf (not in bays) (CTDs WCB 2.2S (Figure 6d), WCB 4.2S (Figure 6f), WCB mooring (Figure 6e)), and in-the-bays (CTDs Rosita Harbour/Bay of Isles (Figure 6c) and Stromness Bay (Figure 6b)). Off-shelf waters are the least concentrated in CH_4 on average throughout the water column, while bay waters are the most concentrated. The average CH_4 concentration of all samples taken throughout the water column off the South Georgia shelf is 3.74 ± 0.35 nmol/L, the average on-shelf of South Georgia (not in bays) is 5.39 ± 0.37 nmol/L, and the average in-the-bays of South Georgia is 10.23 ± 0.84 nmol/L. CH_4 concentrations are elevated throughout the water column in the bays (Figure 6),

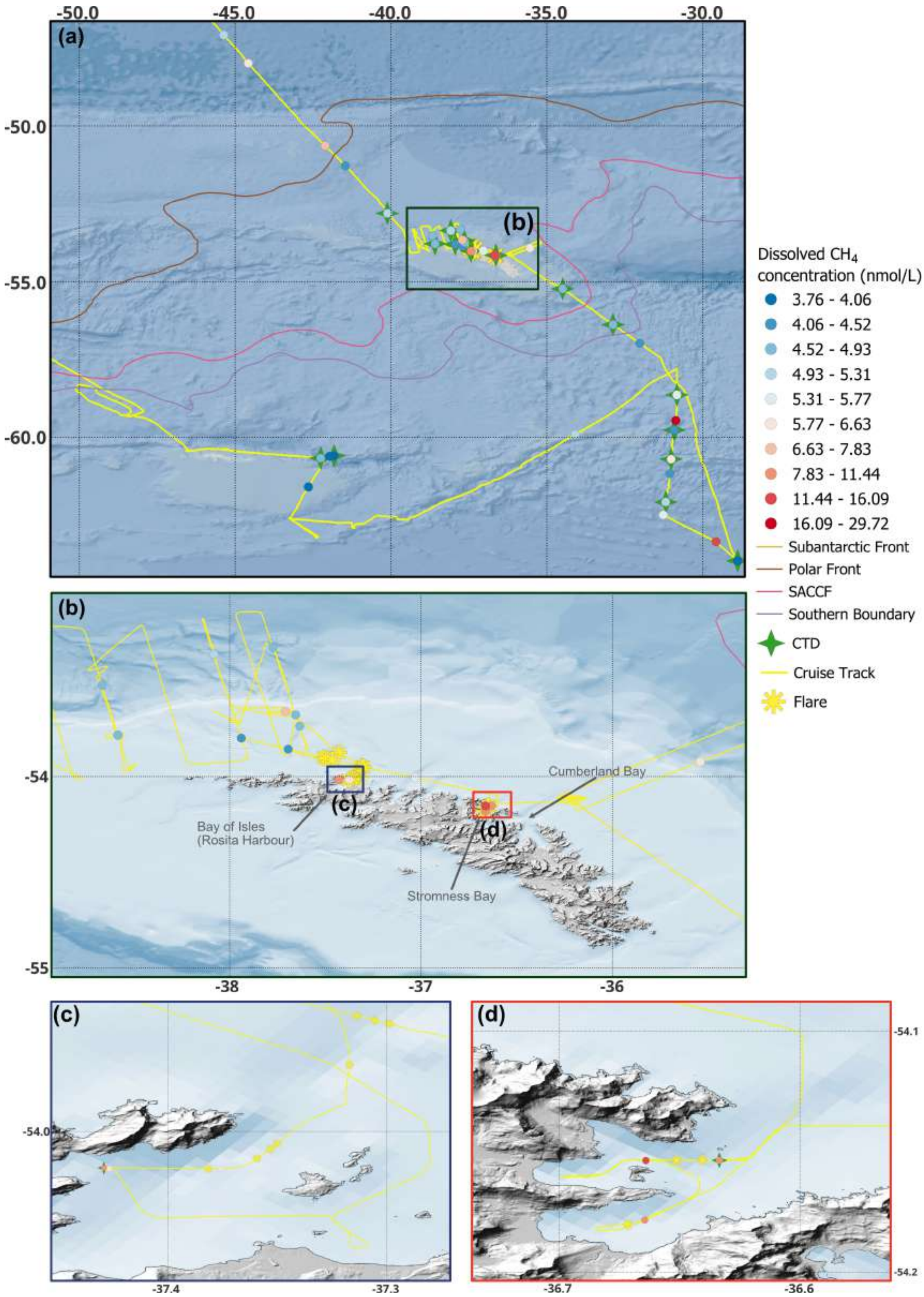

Figure 3. Sea surface dissolved CH_4 concentration (blue/white/red circles), with the concentration indicated by the colours in the scale, (a) in the study area, (b) South Georgia shelf, (c) Bay of Isles, and (d) Stromness Bay. The yellow track represents the cruise track, green stars in (a) represent location of CTD casts, yellow stars in (b), (c) and (d) represent location of flares detected in this study.

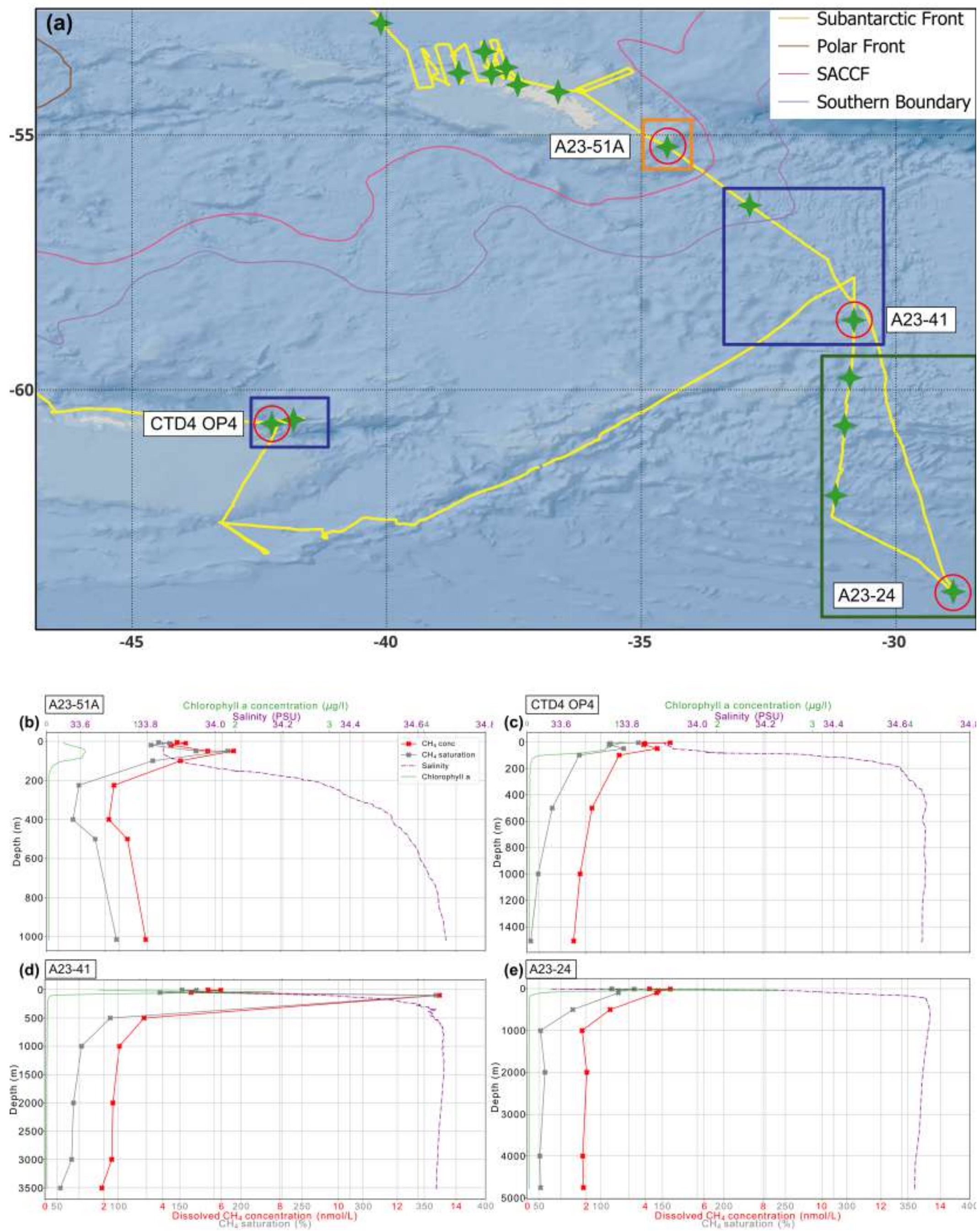

Figure 4. (a) Location of CTD casts (green stars) taken for dissolved CH_4 concentrations throughout the study. The profiles of CTD casts circled in red are shown in (b)-(e). CTD cast in orange rectangle is in the ACC, CTD casts in blue rectangles are in the Weddell-Scotia Confluence, and the CTD casts in green rectangle are in the Weddell Gyre. The yellow line indicates the cruise track. The brown, pink and purple lines represent oceanographic front: Polar Front, Southern Antarctic Circumpolar Current Front, and the southern boundary of the Polar Front, respectively, as indicated in the legend. (b)-(e) Water column profiles of dissolved CH_4 concentrations (red), CH_4 saturation (grey), chlorophyll a concentrations (green) and salinity (purple) at CTDs: (b) A23-51, (c) CTD4 OP4, (d) A23-41, (e) and A23-24.

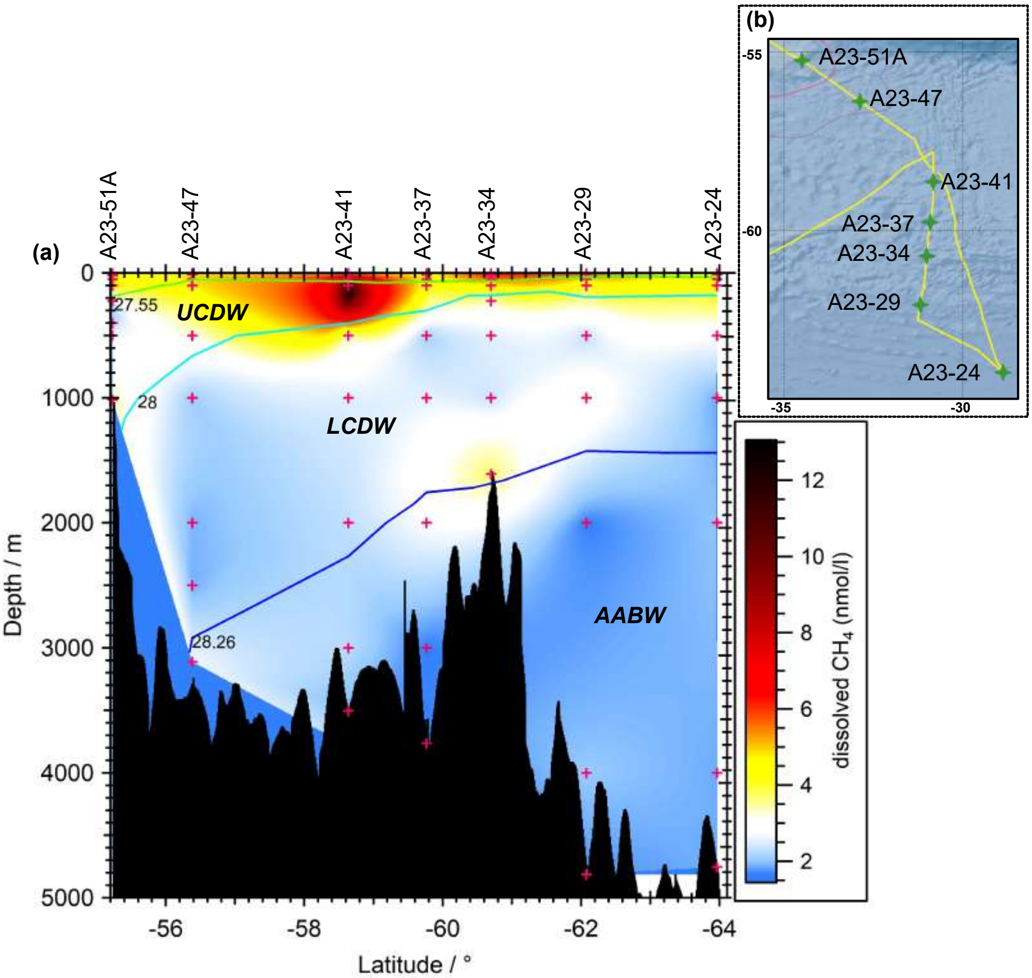

Figure 5. (a) Dissolved methane concentrations in the Scotia and Weddell Seas along the A23 transect. Data is collected from 7 CTD casts (indicated above the graph) with 8 to 9 depths sampled at each cast location (red crosses). The data is interpolated across the whole space. Isopycnals of neutral density are marked on in green (27.55 kg/m^3), light blue (28 kg/m^3) and dark blue (28.26 kg/m^3) lines, and these mark the boundaries of the different water masses: Antarctic Bottom Water (AABW), Lower Circumpolar Deep Water (LCDW) and Upper Circumpolar Deep Water (UCDW). The seabed is in black. (b) A23 transect with CTD casts sampled in this study (and depicted in (a)) indicated by green stars, and cruise track indicated by yellow line.

compared to on-shelf. The waters just off shelf of South Georgia (CTD WCB 3.2N) are not elevated in CH_4 compared to the mean off-shelf CH_4 concentrations throughout the water column over the entire study area (3.72 ± 0.18 nmol/L), indicating that the CH_4 enriched waters are confined to the South Georgia shelf.

Water column profiles on the South Georgia shelf either show elevated CH_4 concentrations near the sediment surface and decreasing towards the ocean surface (i.e. Stromness Bay (Figure 6b) and WCB mooring CTDs (Figure 6e)), or more constant throughout the water column (i.e. Rosita (Figure 6c), WCB 2.2S (Figure 6d), and WCB 4.2S CTDs (Figure 6f)). In waters just off the South Georgia shelf, deeper waters are more depleted in CH_4 and concentrations increase towards the ocean surface (Figure 6g). Note that the CTD in Stromness was deployed approximately over the site of a flare identified using EK80 echosounder (Figure S2 Supporting information).

Gas flares were found during flare surveys on 4^{th} and 5^{th} January 2023 in Bay of Isles, Stromness Bay and on the South Georgia shelf (Figure 6a). Flares were only detected using the single beam (EK80) echosounder. The shallow water multibeam echosounder (EM710) did not detect any flares, potentially because the frequency (100 kHz) was too high. Therefore, the area of seafloor that we were able to search is limited to directly below the ship's path. While there were flares present both on-shelf and in-the-bays (Figure 6a), there is only significant increase in surface water CH_4 concentration in-the-bays (Bay of Isles (Rosita CTD) ((Figure 6b) and Stromness Bay) (Figure 6c)). The water depths corresponding to the locations of the in-bay CTD casts range from 59 m to 120 m, and for the on-shelf CTD casts, 135 m to 310 m.

3.4 Sea-air Methane Fluxes

Sea-air CH_4 fluxes for both off-shelf and on-shelf regions were calculated after removing surface water concentration outliers (see Section 3.2). The mean sea-air CH_4 flux across the off-shelf Scotia and Weddell seas was calculated to be 0.136 ± 0.021 $\mu\text{mol}\,\text{m}^{-2}\,\text{d}^{-1}$, while across the South Georgia shelf it was calculated to be 0.269 ± 0.035 $\mu\text{mol}\,\text{m}^{-2}\,\text{d}^{-1}$. On the South Georgia shelf, the largest flux was calculated in Stromness Bay (Figure 7d), which coincided with the highest surface water CH_4 concentrations on the shelf (Figure 3d). The average sea-air flux in South Georgia's bays was calculated to be 0.336 ± 0.04 $\mu\text{mol}\,\text{m}^{-2}\,\text{d}^{-1}$. In the open ocean, the mean flux was 0.236 ± 0.021 $\mu\text{mol}\,\text{m}^{-2}\,\text{d}^{-1}$north of the SACCF, and 0.131 ± 0.022 $\mu\text{mol}\,\text{m}^{-2}\,\text{d}^{-1}$south of the SACCF, indicating that, while all areas of the study area show CH_4 release to the atmosphere, more CH_4 is released north of the SACCF than south.

4 Discussion

4.1 Seabed and ocean methane

4.1.1 Weddell Sea and Scotia Sea

In the deep water masses of the Weddell and Scotia seas, CH_4 concentrations were significantly lower than those at the surface, with the lowest concentrations found in the deepest water mass, Antarctic bottom water (AABW). CH_4 concentrations increased progressively in the shallower water masses, with higher values in Lower Circumpolar Deep Water (LCDW) and Upper Circumpolar Deep Water (UCDW). This pattern aligns with the findings of Heeschen et al. (2004), which identified air/ocean exchange as the primary CH_4 source in these regions. The turnover time for Antarctic Bottom Water (AABW) in this area is approximately 16 years (Heeschen et al., 2004), indicating that these deep waters last interacted with the atmosphere in the years 2006 and/or 2007. Our results may indicate that there has been an increase in CH_4 concentrations in the Weddell Sea throughout the whole water column since observations by Heeschen et al. (2004) which

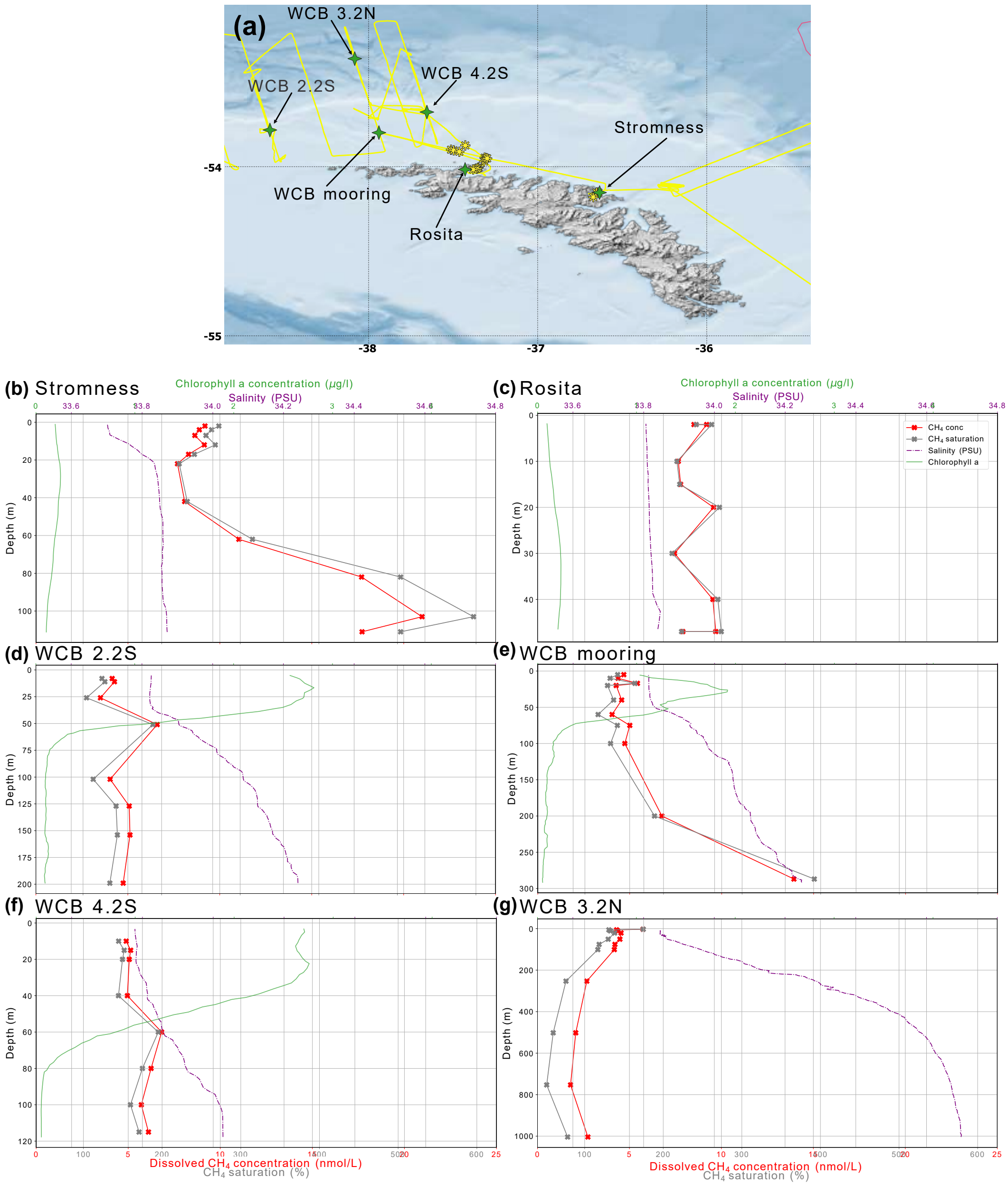

Figure 6. (a) Location of CTD casts (green stars) taken for dissolved CH_4 concentrations around South Georgia and CH_4 flares found in this study (yellow stars). Cruise track is indicated by yellow line. (b)-(g) water column profiles of dissolved CH_4 concentrations (red), CH_4 saturation (grey), chlorophyll a concentrations (green) and salinity (purple) at CTDs: (b) Stromness, (c) Rosita, (d) WCB 2.2S, (e) WCB mooring, (f) WCB 4.2S, and (g) WCB 3.2N. Note that the scale of the y-axis (depth) is different for (b)-(g), each CTD cast reaches to the seafloor.

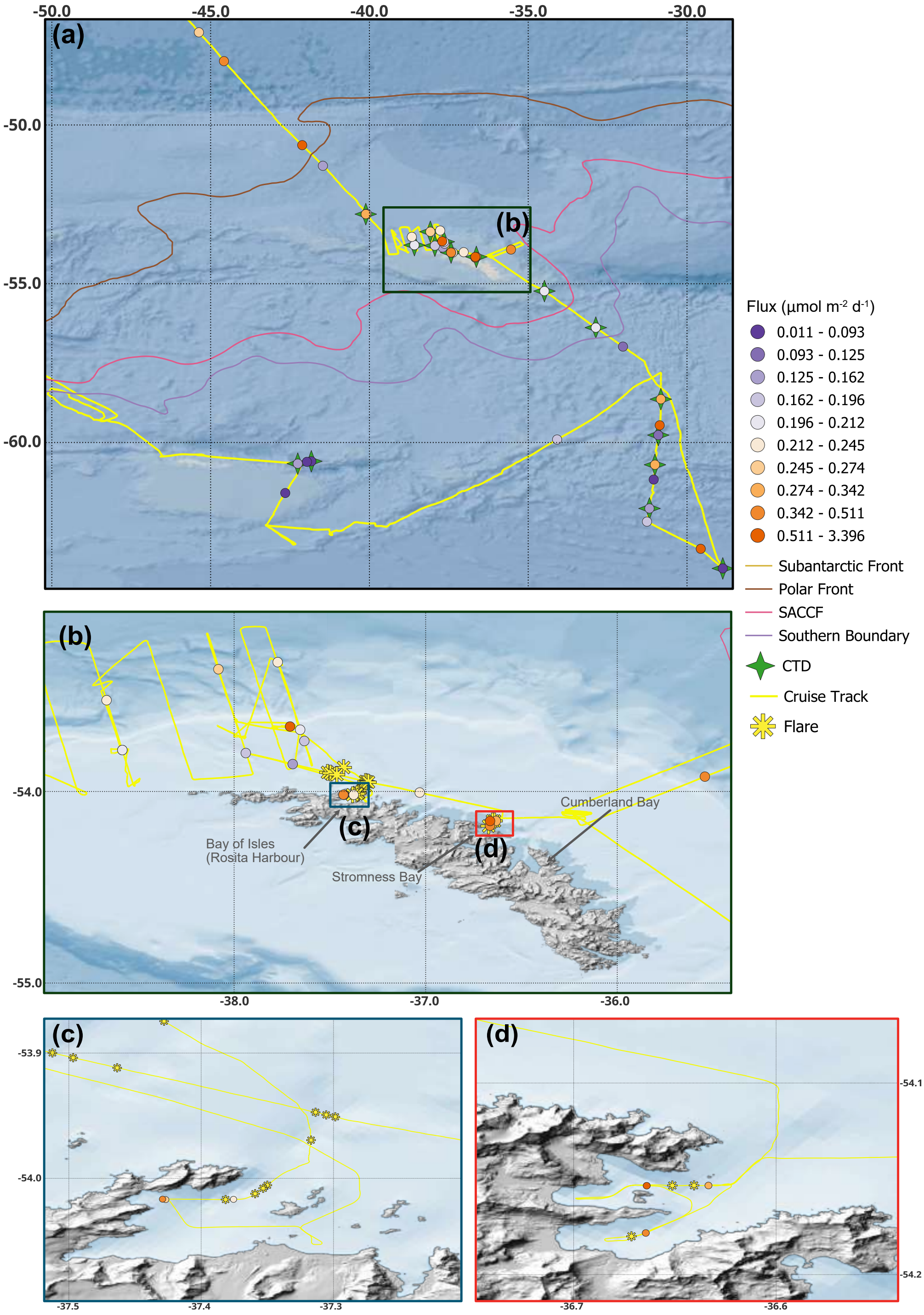

Figure 7. Sea-air CH_4 fluxes calculated (a) across the study area, (b) zoomed into South Georgia Island, (c) zoomed into Bay of Isles, South Georgia, and (d) zoomed into Stromness Bay, South Georgia. Each circle represents a flux calculation with the colour indicating the size of the flux as shown in the scale. All fluxes indicate CH_4 travelling from sea to the atmosphere. Yellow stars in (c) and (d) indicate the location of flare found in this study. The yellow track in (c) and (d) is the cruise track.

were made 25 years prior to this study. Given that atmospheric exchange was identified as the main CH_4 source in the Weddell Sea by Heeschen et al. (2004), this increase may reflect rising atmospheric CH_4 concentrations over the past 25 years. However, the percentage increase in AABW CH_4 concentration between Heeschen et al. (2004) and our study (between 136% and 339%, when comparing averages across similar regions) exceeds the atmospheric increase over that time period ($\sim$ 109%, when compared with data collected at corresponding dates at Palmer station as part of the NOAA Cooperative Global Air Sampling Network (Global Monitoring Laboratory, 2024)), suggesting additional factors, such as changes in oceanographic processes, sedimentation or regional climate conditions, may be influencing CH_4 dynamics. However, the discrepancy in dissolved CH_4 concentration in bottom water masses between this study and Heeschen et al. (2004) may be a result of analytical differences between different laboratories. Wilson et al. (2018) demonstrate that results from different laboratories can be significantly different, meaning it is difficult to compare results from one laboratory with another.

The water column profiles in the Weddell and Scotia seas show an increase in CH_4 concentration at $\sim$ 100 m. This sub-surface CH_4 maxima occasionally corresponds with a maxima in chlorophyll a concentration (e.g. Figures 4b and 4e). An increase in the concentration of phytoplankton at this depth could explain the coincident increase in CH_4, as phytoplankton have been found to produce methane in oxygen-rich upper waters of the ocean during the process of photosynthesis (Lenhart et al., 2016; Klintzsch et al., 2019, 2020; Bižić et al., 2020; Bižić, 2021). However, not all the subsurface CH_4 maxima correspond with an increase in chlorophyll a, meaning there is another unexplained reason for the elevated CH_4 concentrations at this depth.

4.1.2 South Georgia

The South Georgia on-shelf waters exhibited distinct CH_4 profiles compared to off-shelf regions in the Weddell and Scotia seas. On-shelf profiles show evidence of seabed CH_4 production, as indicated by increased CH_4 concentrations near the seabed (Figures 6b and 6e) or relatively constant CH_4 concentrations throughout the water column (Figures 6c, 6d and 6f). The presence of CH_4 flares in this area found in this study (Figure 6a), and of small pock marks, bacterial mats and rising methane gas bubbles in previous studies (Römer et al., 2014; Geprägs et al., 2016; Bohrmann et al., 2017), further supports the presence of seabed CH_4 production and release. The average CH_4 concentration throughout the water column on-shelf is higher than the average off-shelf, indicating that the South Georgia on-shelf waters are more CH_4-enriched compared to the open ocean waters. Even just off the South Georgia shelf (CTD WCB 2.2N, Figure 6g), the mean CH_4 concentration is not significantly different from the mean off-shelf CH_4 concentration across the entire study area. These results suggest that elevated CH_4 concentrations in the water column and seabed CH_4 production and release is largely confined to the South Georgia shelf.

South Georgia's bays exhibit higher CH_4 saturation throughout the water column compared to the on-shelf waters, with greater amounts of CH_4 reaching the surface in the bays. The shallower waters of the bays allow more seabed CH_4 to reach the surface, as less is oxidized in the water column as it travels to the surface. The bays of South Georgia may have higher flare activity, which would result in higher concentrations of CH_4 throughout the water column, including at the seafloor, compared to the other on-shelf regions. In this study, we identify a greater density of flares in the bays compared to other areas, however, the acoustic survey focused preferentially on bay areas, potentially leading to a higher detection rate of CH_4 flares in bays. Alternatively, the CH_4 saturated water may be more confined in the bays rather than diffused by currents as on the shelf, further exacerbating the localised CH_4 enrichment in the bay waters.

4.2 Ocean to atmosphere

Oceanic CH_4 is linked to the atmosphere through the surface layer (sea-air interface). All the surface waters across the region are super-saturated with CH_4 with respect to the atmosphere, and hence an atmospheric CH_4 source. Surface water CH_4 concentrations showed significant spatial variation, with higher concentrations on the South Georgia shelf compared to off-shelf waters. This observation is consistent with previous studies (Bange et al., 1994; Weber et al., 2019) which investigate fluxes on a global scale, and suggests that shelf regions are sources of CH_4. A latitudinal gradient in surface CH_4 concentrations was observed, decreasing going south across the SACCF. This observation is likely driven by the upwelling of cold, CH_4-depleted waters in the Antarctic Circumpolar Current (ACC) (Heeschen et al., 2004; Yoshida et al., 2011; Bui et al., 2018; Weber et al., 2019). Upwelling brings deep, CH_4-depleted waters to the surface, reducing surface CH_4 concentrations. Therefore, seabed depth and latitude are important parameters in determining the distribution of CH_4 in surface waters in this region of the South Atlantic and Southern Oceans. Previous studies have found the main processes controlling CH_4 distribution in the Southern Ocean to be vertical mixing (upwelling) and sea-air exchange (Heeschen et al., 2004; Yoshida et al., 2011; Bui et al., 2018).

Sea-air CH_4 fluxes link surface water and atmospheric CH_4 concentrations, allowing us to assess the overall impact of the ocean on atmospheric CH_4 levels. This study finds the study region of the South Atlantic and Southern Oceans to be a small source of CH_4, with on-shelf sea-air CH_4 fluxes of 0.269 ± 0.035 µmol m^{-2} d^{-1}and off-shelf fluxes of 0.136 ± 0.021 µmol m^{-2} d^{-1}. Previous studies have found contrasting results regarding the role the Southern Ocean plays in the atmospheric CH_4 cycle; some studies identify the Southern Ocean as a source of CH_4, while others find it to be a sink. Ye et al. (2023) found the Ross Sea to be a CH_4 sink, with a negative sea-air flux. Similarly, Heeschen et al. (2004) reported the Weddell Sea as a CH_4 sink. Tilbrook and Karl (1994) found the Drake Passage to be a CH_4 sink, whereas the South Shetland Islands and Bransfield Strait were sources, indicated by a positive sea-air flux. Yoshida et al. (2011) observed that areas south of the polar front (between 54°S and 65°S) were CH_4 sources during December, January, and February, with mean fluxes ranging from 0.8 to 2.1 µmol m^{-2} d^{-1}. Bui et al. (2018) also found the Southern Ocean to be a CH_4, source during these months, although with smaller fluxes than those reported by Yoshida et al. (2011). Workman, Fisher, et al. (2024) found off-shelf regions of the Southern Ocean to be a small CH_4 sinks, while on-shelf regions were CH_4 sources.

In this study, the highest average sea-air CH_4 fluxes were observed on the South Georgia shelf, particularly in the bay areas, which this study also finds to have elevated surface water CH_4 concentrations compared to other areas. The presence of methane flares and elevated CH_4 in the water column indicates active seabed sources that may enhance the flux of CH_4 from the sea to the atmosphere. Workman, Fisher, et al. (2024) found the South Georgia shelf to be a source of CH_4 with an average sea-air flux of 7.34 ± 1.54 µmol m^{-2} d^{-1}, which is at least an order of magnitude greater than the fluxes found in this study. This discrepancy could be due to different flux measurement techniques; Workman, Fisher, et al. (2024) used the eddy-covariance method, which can detect direct emissions of CH_4 (e.g. ebullition) and diffusive fluxes, whereas this study used the bulk flux method, which accounts only for diffusive fluxes, emphasising the significance of ebullition in shallow waters to drive sea-air CH_4 fluxes.

In contrast, off-shelf regions exhibited lower (but still positive) sea-air CH_4 fluxes, attributed to lower CH_4 surface water concentrations due to fewer CH_4 sources. Within the off-shelf area, fluxes varied across different oceanographic regions. For instance, regions influenced more by upwelling, such as those south of the Southern Antarctic Circumpolar Current Front (SACCF), showed lower sea-air CH_4 fluxes as upwelling of cold, CH_4-depleted waters reduces surface CH_4 concentrations, as described earlier, hence limiting the amount of CH_4 available for emission to the atmosphere.

By integrating sea-air CH_4 flux data with surface and atmospheric CH_4 measurements, we can better understand the contribution of the Southern Ocean and South Atlantic to the global CH_4 cycle. These fluxes provide a crucial link between oceanic and atmospheric CH_4, highlighting the importance of on-shelf and oceanographic processes, like upwelling, in controlling CH_4 oceanic emissions.

Based on the fluxes calculated in this study, we estimate the amount of CH_4 released from the Scotia Sea, Weddell Sea and South Georgia shelf to be 0.043 ± 0.039 Gg per month. Extrapolating this to one year, the CH_4 emissions amount to ∼ 0.00009 % of the total annual global CH_4 emissions (Saunois et al., 2024). However, there is likely seasonal variability in the emission of CH_4 from this region due to the presence of sea-ice acting as a barrier to sea-air exchange (James et al., 2016). Therefore, scaling up the summertime emissions calculated here to the whole year may overestimate the yearly emissions due to sea-ice extent being lowest in summer. Therefore, 0.00009% of the global methane budget is likely an overestimate for this area.

4.3 Factors impacting atmospheric concentrations

Atmospheric CH_4 concentrations measured during this study are mainly impacted by long range transport. For example, for the first three days of the study (22nd to 25th December 2022) the detrended atmospheric concentration residuals are lower than the NOAA baseline due to air masses originating from the Atlantic Ocean. Whereas during the rest of the cruise the air masses originate from the opposite direction (from the west/south-west), from the southern tip of South America/Drake Passage. This could explain the discrepancy in the atmospheric concentrations; there are limited CH_4 sources from the mid Atlantic Ocean, while there are more CH_4 sources from terrestrial South America (e.g. agricultural, wetlands, fossil fuel burning). The sustained elevated atmospheric CH_4 concentrations over the South Georgia shelf could be attributed to more local CH_4 emissions rather than long range transport, due to presence of local CH_4 emissions on the South Georgia shelf.

4.4 Localised source: South Georgia

This study identifies the South Georgia shelf as a localised source of CH_4 due to raised CH_4 concentrations throughout the on-shelf and in-the-bays water columns compared to off-shelf regions. This results in increased CH_4 release from the waters of the South Georgia shelf into the atmosphere. There is a clear link between seabed production of CH_4, the CH_4 concentration at the surface and the amount of CH_4 released into the atmosphere. More CH_4 reaches the surface waters in bays, and hence more CH_4 reaches the atmosphere from the bay waters. This may be due to more potential CH_4 sources in bays (i.e. seabed seepage, freshwater outflow) or that the CH_4 enriched water is confined in the bays, restricting its movement, as discussed in section 3.2. Römer et al. (2014) and Geprägs et al. (2016) find that the seabed CH_4 of the South Georgia shelf has a biogenic origin, based on isotopic measurements of sedimentary gas.

Stromness Bay exhibits particularly high CH_4 concentrations throughout the water column compared to other areas (Figure 6b). The Stromness CTD, deployed over a suspected flare location (see Figure S2 in SI), showed a CH_4 concentration profile indicating seabed CH_4 production, with the highest concentrations near the seabed. Stromness Bay is also associated with the greatest sea-air flux and surface concentration on the South Georgia shelf, making clear the link between seabed CH_4 and emission to the atmosphere. The origin of the seabed CH_4 in Stromness Bay was not investigated in this study, so therefore not known. However, Römer et al. (2014) and Geprägs et al. (2016) find that seabed CH_4 in Cumberland Bay is of a microbial origin, based on isotope analysis of CH_4 from sediment gas samples. We can hypothesise that the seabed CH_4 in Stromness Bay likely has similar origin due to proximity to Cumberland Bay. Additionally, Römer et al. (2014) also finds that CH_4 in sediments in a trough outside of bays is of microbial origin, making a stronger case for Stromness Bay having microbially originated CH_4.

In the Stromness Bay water column profile there is a slight increase in CH_4 concentration towards the surface, corresponding with a decrease in salinity (Figure 6b), suggesting that CH_4-enriched freshwater from glacial melt could be contributing to surface layer CH_4. Danis et al. (2024) found that marine-terminating glaciers are a significant source of CH_4 in surface waters off the West Antarctic Peninsula, more so than land-terminating glaciers. Although the glaciers surrounding Stromness Bay are land-terminating, CH_4-enriched freshwater could still enter the surface waters via streams and rivers. While glacier meltwater may be a source of CH_4 in Stromness Bay in this study, Geprägs et al. (2016) find that there is no evidence that glacier meltwater contributes to the CH_4 in neighbouring bay, Cumberland Bay.

The CH_4 water column profile of WCB mooring (Figure 6e) is also characteristic of seabed CH_4 release, as evident from the increased dissolved CH_4 concentration close to the seabed. The atmospheric concentration above WCB mooring is also elevated (Figure 2), which could indicate a local oceanic source of atmospheric CH_4. However, the sea-air flux calculated using the dissolved CH_4 concentrations in the surface water is not elevated at the location of WCB mooring. This could indicate that seabed CH_4 is transported to the atmosphere primarily directly (e.g. ebullition), rather than by diffusion, or that the elevated CH_4 concentration air has travelled from elsewhere.

We observed a peak in the 2-hourly atmospheric CH_4 seasonally detrended residuals (Figure 2c) over the South Georgia shelf. Back trajectories for air masses over this period of elevated CH_4 concentrations show that the air mass originated from different directions throughout the period. This may indicate that the source of the CH_4 is local. There are 2 bases on South Georgia, King Edward Point (KEP) and Bird Island (BI) (Figure 1), with populations during the time period of elevated CH_4 concentrations over the South Georgia shelf (3^{rd} to 6^{th} January 2023) of 14-20 and 4, respectively. With such small numbers populating these bases, we wouldn't expect emissions to be seen by the ship. Additionally, the back trajectories corresponding to the elevated CH_4 concentrations originate from north/west, which is away from the larger base at KEP. There was 1 cruise ship around the island during the period 3^{rd} to 6^{th} January 2023 (the length of ship was 104 m). During the period of elevated atmospheric CH_4 concentrations the cruise ship was in the Bay of Isles and travelled south to Stromness Bay, and not upstream of where the air impacting Discovery was coming from (based on the air mass back trajectories (i.e. from the north-west)). The location and information about the cruise ship was obtained through personal correspondence with the Government of South Georgia and South Sandwich Islands (GSGSSI). Therefore, considering the main sources of pollution in the area (research bases and other vessels), we do not expect the atmospheric measurements collected on the South Georgia shelf to be influenced by anthropogenic sources.

There may be other continental or on shore sources of CH_4 to the atmosphere around South Georgia, including penguin and seal colonies on South Georgia Island. Sea animal colonies have previously been found to be a source of atmospheric CH_4 (R. Zhu et al., 2009). There is a large king penguin colony in Bay of Isles (Salisbury Plain), this is a breeding site with as many as 60,000 king penguin breeding pairs (Clarke et al., 2012) and is one of the largest king penguin colonies on South Georgia. Additionally there are large populations of fur and elephant seals in the north of the island, including at Bird Island, Undine Bay, Right Whale Bay and Bay of Isles (Boyd, 1993). These sea animal colonies could be causing elevated CH_4 concentrations detected by the ship.

The elevated atmospheric CH_4 concentrations above the South Georgia shelf may originate from a local oceanic source. We have observed elevated sea-air CH_4 fluxes on the shelf and seen evidence of seabed CH_4 seeps, supporting the presence of a local oceanic

CH_4 source in this area. However, there are other potential sources of CH_4 in the area which could explain the increased atmospheric CH_4 concentrations, including the large seal and penguin colonies in the area (northern part of South Georgia). It difficult within the scope of this study to identify the source of elevated CH_4. Also, it is important to note that the increase in atmospheric concentrations over the South Georgia shelf compared to over open ocean areas, are very small, corresponding to 3 to 5 ppb.

5 Conclusions

This study provides a characterisation of methane in the Southern Ocean and South Atlantic region, linking CH_4 in surface waters, deep water masses, and in the atmosphere through sea-air fluxes. We investigated both on-shelf (South Georgia) and off-shelf, open waters in this study and it is the first study to link seabed activity (flares) with water column concentrations, sea-air fluxes, and atmospheric concentrations on the South Georgia shelf.

Our results show that the Southern Ocean and South Atlantic are dynamic regions for CH_4 cycling, with spatial variability influenced by upwelling, seabed seepage, and freshwater inputs. We find that CH_4 concentrations are higher in the waters on the South Georgia shelf compared to the open ocean, particularly within the bays of South Georgia, likely due to seabed seepage and freshwater inputs. This highlights the shelf as a key region for methane emissions within the study area. In contrast, open ocean areas of the Scotia and Weddell seas exhibit lower CH_4 fluxes but remain consistent sources of atmospheric methane. The observed increase in CH_4 concentrations in Antarctic bottom and deep waters, compared to measurements from 25 years prior, suggests a shifts in methane dynamics, which may be linked to rising atmospheric CH_4 levels and/or climate-driven changes in ocean conditions.

The results presented in the study suggest that, over the off-shelf regions, the Weddell and Scotia seas are becoming sources of atmospheric methane, releasing more methane into the atmosphere. Currently, we find that the Weddell and Scotia seas contribute minimally to the global methane budget ($\sim 0.00009\%$), however, it is an important result as it represents a switch from sink to source. This switch from sink to source suggested by this study may be an early-warning sign of larger-scale CH_4 release from this region, hence it is important to understand if this trend will continue into the future. To do this, continued monitoring of methane concentrations in the water, air, and continued sea-air flux measurements are necessary. In particular, changing climatic conditions could have major impacts on seabed methane reservoirs, i.e. methane hydrates in the seabed around South Georgia. The potential breakdown of these hydrates due to rising water temperatures could trigger considerably more methane to be emitted from the ocean into the atmosphere, emphasising the importance of continued monitoring of oceanic methane emissions in this region.

Open Research Section

The concentration of atmospheric methane and carbon dioxide and dissolved methane in surface water and water column data used in this study is published with the UK Polar Data Centre (PDC) (Workman, Delille, et al., 2024). The EK80 data used in this study is published with the PDC (Workman, Dornan, & Saunders, 2024). Both datasets are under embargo until this work is published, but editors and reviewers have access to data via login.

Acknowledgments

The authors would like to thank the masters, nautical officers, and all crew members of the research vessel RRS Discovery during expedition DY158. Additionally, we would like to extend a huge thanks to the entire science party of DY158, particularly PSO Dr Ryan Saunders. We would also like to thank Christopher Auckland for consulting on the physical oceanography aspects of this paper, and Dr Povl Abrahamsen for providing advice on oceanic front calculations. Additional thanks goes to Dr Tracey Dornan, Dr Ryan Saunders, Dr Sophie Fielding, and Dr Povl Abrahamsen for help with carrying out the acoustic flare survey on DY158. The authors would like to thank the Neumayer team for supporting the continuous methane measurement, particularly Rolf Weller and Zsófia Jurányi who oversee the atmospheric chemistry programme at Neumayer, and Hannes Keck and Nellie Wullenweber who overwintered during 2022 and 2023 when data used in this work were collected. This work was supported by the Natural Environment Research Council and the ARIES Doctoral Training Partnership (Grant NE/S007334/1). Royal Holloway, University of London thanks NERC for funding through Grants NE/V000780/1 and NE/N016211/1, and the University of Liège thanks F.R.S-FNRS through grants SONATINA (J.0060.22) and SEA ICE SPRAY (T.0061.23). British Antarctic Survey thanks NERC for funding through their MOYA grant NE/N015584/1. Anna E. Jones and Katrin Linse were part of the British Antarctic Survey Polar Science for Planet Earth Programme funded by The Natural Environment Research Council (NERC) and Bruno Delille is a research associate at the F.R.S-FNRS. The ship-based work contributing to this study was funded by the Collaborative Antarctic Science Scheme (CASS).

References

Bange, H. W., Bartell, U. H., Rapsomanikis, S., & Andreae, M. O. (1994, 12). Methane in the Baltic and North Seas and a reassessment of the marine emissions of methane. *Global Biogeochemical Cycles*, *8*(4), 465–480. doi: 10.1029/94gb02181

Berndt, C., Feseker, T., Treude, T., Krastel, S., Liebetrau, V., Niemann, H., ... Steinle, L. (2014, 1). Temporal Constraints on Hydrate-Controlled Methane Seepage off Svalbard. *Science*, *343*(6168), 284–287. doi: 10.1126/science.1246298

Bižić, M. (2021, 10). Phytoplankton photosynthesis: an unexplored source of biogenic methane emission from oxic environments. *Journal of Plankton Research*, *43*(6), 822–830. doi: 10.1093/plankt/fbab069

Bižić, M., Grossart, H., & Ionescu, D. (2020, 2). Methane Paradox. In *Encyclopedia of life sciences* (pp. 1–11). Wiley. doi: 10.1002/9780470015902.a0028892

Bižić-Ionescu, M., Ionescu, D., & Grossart, H. P. (2018, 10). Organic particles: Heterogeneous hubs for microbial interactions in aquatic ecosystems. *Frontiers in Microbiology*, *9*(OCT). doi: 10.3389/fmicb.2018.02569

Bohrmann, G., Aromokeye, A. D., Bihler, V., Dehning, K., Dohrmann, I., Gentz, T., ... Mau, S. (2017). *R/V METEOR Cruise Report M134, Emissions of Free Gas from Cross-Shelf Troughs of South Georgia: Distribution, Quantification, and Sources for Methane Ebullition Sites in Sub-Antarctic Waters, Port Stanley (Falkland Islands) – Punta Arenas (Chile), 16 January – 18 February 2017* (Tech. Rep.).

Boyd, I. L. (1993, 3). Pup production and distribution of breeding Antarctic fur seals (Arctocephalus gazella) at South Georgia. *Antarctic Science*, *5*(1), 17–24. doi: 10.1017/S0954102093000045

Bui, O. T. N., Kameyama, S., Yoshikawa-Inoue, H., Ishii, M., Sasano, D., Uchida, H., & Tsunogai, U. (2018, 1). Estimates of methane emissions from the Southern Ocean from quasi-continuous underway measurements of the partial pressure of methane in surface seawater during the 2012/13 austral summer. *Tellus, Series B: Chemical and Physical Meteorology*, *70*(1), 1–15. doi: 10.1080/16000889.2018.1478594

Burns, R., Wynn, P. M., Barker, P., McNamara, N., Oakley, S., Ostle, N., . . . Stuart, M. (2018, 11). Direct isotopic evidence of biogenic methane production and efflux from beneath a temperate glacier. *Scientific Reports*, *8*(1), 17118. doi: 10.1038/s41598-018-35253-2

Christiansen, J. R., & Jørgensen, C. J. (2018, 11). First observation of direct methane emission to the atmosphere from the subglacial domain of the Greenland Ice Sheet. *Scientific Reports*, *8*(1), 16623. doi: 10.1038/s41598-018-35054-7

Clarke, A., Croxall, J. P., Poncet, S., Martin, A. R., & Burton, R. (2012). Important bird areas: South Georgia. *British Birds*, *105*, 118–144.

Damm, E., Helmke, E., Thoms, S., Schauer, U., Nöthig, E., Bakker, K., . . . Wegener, A. (2010). *Methane production in aerobic oligotrophic surface water in the central Arctic Ocean* (Vol. 7; Tech. Rep.).

Danis, B., Bayat, B., Brusselman, A., Coerper, A., De Borger, E., Delille, B., . . . Wallis, B. (2024). *Report of the TANGO 2 expedition to the West Antarctic Peninsula* (Tech. Rep.). doi: 10.5281/zenodo.11653689

de Boyer Montégut, C., Madec, G., Fischer, A. S., Lazar, A., & Iudicone, D. (2004, 12). Mixed layer depth over the global ocean: An examination of profile data and a profile-based climatology. *Journal of Geophysical Research: Oceans*, *109*(C12). doi: 10.1029/2004JC002378

del Valle, R. A., Yermolin, E., Chiarandini, J., Granel, A. S., & Lusky, J. C. (2017, 2). Methane at the NW of Weddell Sea, Antarctica. *Journal of Geological Research*, *2017*, 1–8. doi: 10.1155/2017/5952916

Dølven, K. O., Ferré, B., Silyakova, A., Jansson, P., Linke, P., & Moser, M. (2022, 2). Autonomous methane seep site monitoring offshore western Svalbard: hourly to seasonal variability and associated oceanographic parameters. *Ocean Science*, *18*(1), 233–254. doi: 10.5194/os-18-233-2022

Formolo, M. (2010). The Microbial Production of Methane and Other Volatile Hydrocarbons. In *Handbook of hydrocarbon and lipid microbiology* (pp. 113–126). Springer Berlin Heidelberg. doi: 10.1007/978-3-540-77587-4{_}6

Forster, P., Storelvmo, T., Armour, K., Collins, W., Dufresne, J.-L., Frame, D., . . . Zhang, H. (2021). The Earth's Energy Budget, Climate Feedbacks, and Climate Sensitivity. In V. Masson-Delmotte et al. (Eds.), *Climate change 2021: The physical science basis. contribution of working group i to the sixth assessment report of the intergovernmental panel on climate change* (chap. 7). Cambridge, UK and New York, NY, USA: Cambridge University Press. doi: 10.1017/9781009157896.009

Fox-Kemper, B., Hewitt, H. T., Xiao, C., Aðalgeirsdóttir, G., Drijfhout, S. S., Edwards, T. L., . . . Yu, Y. (2021). Ocean, Cryosphere and Sea Level Change. In V. Masson-Delmotte et al. (Eds.), *Climate change 2021: The physical science basis. contribution of working group i to the sixth assessment report of the intergovernmental panel on climate change* (chap. 9). Cambridge, UK and New York, NY, USA: Cambridge University Press. doi: 10.1017/9781009157896.011

Geprägs, P., Torres, M. E., Mau, S., Kasten, S., Römer, M., & Bohrmann, G. (2016, 4). Carbon cycling fed by methane seepage at the shallow Cumberland Bay, South Georgia, sub-Antarctic. *Geochemistry, Geophysics, Geosystems*, *17*(4), 1401–1418. doi: 10.1002/2016GC006276

Global Monitoring Laboratory. (2024). *Cooperative Air Sampling Network.* Retrieved from `https://gml.noaa.gov/ccgg/flask.html`

Graves, C. A., Steinle, L., Rehder, G., Niemann, H., Connelly, D. P., Lowry, D., . . . James, R. H. (2015, 9). Fluxes and fate of dissolved methane released at the seafloor at the landward limit of the gas hydrate stability zone offshore western Svalbard. *Journal of Geophysical Research: Oceans*, *120*(9), 6185–6201. doi: 10.1002/2015jc011084

Heeschen, K. U., Keir, R. S., Rehder, G., Klatt, O., & Suess, E. (2004, 6). Methane dynamics in the Weddell Sea determined via stable isotope ratios and CFC-11. *Global Biogeochemical Cycles*, *18*(2), n/a–n/a. doi: 10.1029/2003gb002151

Heywood, K. J., Schmidtko, S., Heuzé, C., Kaiser, J., Jickells, T. D., Queste, B. Y., ... Smith, W. (2014, 7). Ocean processes at the Antarctic continental slope. *Philosophical Transactions of the Royal Society A: Mathematical, Physical and Engineering Sciences*, *372*(2019), 20130047. doi: 10.1098/rsta.2013.0047

Hinrichs, K.-U., & Boetius, A. (2002). The Anaerobic Oxidation of Methane: New Insights in Microbial Ecology and Biogeochemistry. In *Ocean margin systems* (pp. 457–477). Springer Berlin Heidelberg. doi: 10.1007/978-3-662-05127-6{_}28

Ho, D. T., Law, C. S., Smith, M. J., Schlosser, P., Harvey, M., & Hill, P. (2006, 8). Measurements of air-sea gas exchange at high wind speeds in the Southern Ocean: Implications for global parameterizations. *Geophysical Research Letters*, *33*(16). Retrieved from https://onlinelibrary.wiley.com/doi/full/10.1029/2006GL026817https://onlinelibrary.wiley.com/doi/abs/10.1029/2006GL026817https://agupubs.onlinelibrary.wiley.com/doi/10.1029/2006GL026817 doi: 10.1029/2006GL026817

Jähne, B., Heinz, G., & Dietrich, W. (1987, 9). Measurement of the diffusion coefficients of sparingly soluble gases in water. *Journal of Geophysical Research: Oceans*, *92*(C10), 10767–10776. doi: 10.1029/JC092iC10p10767

James, R. H., Bousquet, P., Bussmann, I., Haeckel, M., Kipfer, R., Leifer, I., ... Greinert, J. (2016, 11). *Effects of climate change on methane emissions from seafloor sediments in the Arctic Ocean: A review* (Vol. 61). Wiley Blackwell. doi: 10.1002/lno.10307

Karl, D. M., Beversdorf, L., Björkman, K. M., Church, M. J., Martinez, A., & Delong, E. F. (2008, 6). Aerobic production of methane in the sea. *Nature Geoscience*, *1*(7), 473–478. doi: 10.1038/ngeo234

Klintzsch, T., Langer, G., Nehrke, G., Wieland, A., Lenhart, K., & Keppler, F. (2019, 10). Methane production by three widespread marine phytoplankton species: release rates, precursor compounds, and potential relevance for the environment. *Biogeosciences*, *16*(20), 4129–4144. doi: 10.5194/bg-16-4129-2019

Klintzsch, T., Langer, G., Wieland, A., Geisinger, H., Lenhart, K., Nehrke, G., & Keppler, F. (2020, 9). Effects of Temperature and Light on Methane Production of Widespread Marine Phytoplankton. *Journal of Geophysical Research: Biogeosciences*, *125*(9). doi: 10.1029/2020jg005793

Knies, J., Damm, E., Gutt, J., Mann, U., & Pinturier, L. (2004, 6). Near-surface hydrocarbon anomalies in shelf sediments off Spitsbergen: Evidences for past seepages. *Geochemistry, Geophysics, Geosystems*, *5*(6). doi: 10.1029/2003gc000687

Lamarche-Gagnon, G., Wadham, J. L., Sherwood Lollar, B., Arndt, S., Fietzek, P., Beaton, A. D., ... Stibal, M. (2019, 1). Greenland melt drives continuous export of methane from the ice-sheet bed. *Nature*, *565*(7737), 73–77. doi: 10.1038/s41586-018-0800-0

Lenhart, K., Klintzsch, T., Langer, G., Nehrke, G., Bunge, M., Schnell, S., & Keppler, F. (2016, 6). Evidence for methane production by the marine algae Emiliania huxleyi. *Biogeosciences*, *13*(10), 3163–3174. doi: 10.5194/bg-13-3163-2016

Manning, C., & Nicholson, D. (2022). *dnicholson/gas_toolbox: MATLAB code for calculating gas fluxes. Zenodo.* doi: 10.5281/zenodo.6126685

Mau, S., Römer, M., Torres, M. E., Bussmann, I., Pape, T., Damm, E., ... Bohrmann, G. (2017, 2). Widespread methane seepage along the continental margin off Svalbard - from Bjørnøya to Kongsfjorden. *Scientific Reports*, *7*(1). doi: 10.1038/srep42997

McGinnis, D. F., Greinert, J., Artemov, Y., Beaubien, S. E., & Wüest, A. (2006).

Fate of rising methane bubbles in stratified waters: How much methane reaches the atmosphere? *Journal of Geophysical Research*, *111*(C9). doi: 10.1029/2005jc003183

Meredith, M. P., Povl Abrahamsen, E., Alexander Haumann, F., Leng, M. J., Arrowsmith, C., Barham, M., ... Tarling, G. A. (2023, 6). Tracing the impacts of recent rapid sea ice changes and the A68 megaberg on the surface freshwater balance of the Weddell and Scotia Seas. *Philosophical Transactions of the Royal Society A: Mathematical, Physical and Engineering Sciences*, *381*(2249). doi: 10.1098/rsta.2022.0162

Milkov, A. V. (2005, 5). Molecular and stable isotope compositions of natural gas hydrates: A revised global dataset and basic interpretations in the context of geological settings. *Organic Geochemistry*, *36*(5), 681–702. doi: 10.1016/j.orggeochem.2005.01.010

Naveira Garabato, A. C., Heywood, K. J., & Stevens, D. P. (2002). *Modification and pathways of Southern Ocean Deep Waters in the Scotia Sea* (Vol. 49; Tech. Rep.).

Park Young-Hyang, D. I. (2019). *Altimetry-drived Antarctic Circumpolar Current fronts.* doi: 10.17882/59800

Polonik, N. S., Ponomareva, A. L., Eskova, A. I., Shakirov, R. B., Obzhirov, A. I., & Morozov, E. G. (2021, 11). Distribution and Sources of Methane in the Water Layers of the Antarctic Straits: Bransfield Strait and Antarctic Sound. *Oceanology*, *61*(6), 892–898. doi: 10.1134/S0001437021060308

Rajan, A., Mienert, J., & Bünz, S. (2012, 4). Acoustic evidence for a gas migration and release system in Arctic glaciated continental margins offshore NW-Svalbard. *Marine and Petroleum Geology*, *32*(1), 36–49. doi: 10.1016/j.marpetgeo.2011.12.008

Reeburgh, W. S. (1980, 5). Anaerobic methane oxidation: Rate depth distributions in Skan Bay sediments. *Earth and Planetary Science Letters*, *47*(3), 345–352. doi: 10.1016/0012-821x(80)90021-7

Repeta, D. J., Ferrón, S., Sosa, O. A., Johnson, C. G., Repeta, L. D., Acker, M., ... Karl, D. M. (2016, 12). Marine methane paradox explained by bacterial degradation of dissolved organic matter. *Nature Geoscience*, *9*(12), 884–887. doi: 10.1038/ngeo2837

Römer, M., Torres, M., Kasten, S., Kuhn, G., Graham, A. G. C., Mau, S., ... Bohrmann, G. (2014, 10). First evidence of widespread active methane seepage in the Southern Ocean, off the sub-Antarctic island of South Georgia. *Earth and Planetary Science Letters*, *403*, 166–177. doi: 10.1016/j.epsl.2014.06.036

Royer, S. J., Ferrón, S., Wilson, S. T., & Karl, D. M. (2018, 8). Production of methane and ethylene from plastic in the environment. *PLoS ONE*, *13*(8). doi: 10.1371/journal.pone.0200574

Ruppel, C. D. (2011). Methane Hydrates and Contemporary Climate Change. *Nature Education Knowledge*, *3(10)*, 29.

Ruppel, C. D., & Kessler, J. D. (2017, 2). The interaction of climate change and methane hydrates. *Reviews of Geophysics*, *55*(1), 126–168. doi: 10.1002/2016rg000534

Sahling, H., Römer, M., Pape, T., Bergès, B., dos Santos Fereirra, C., Boelmann, J., ... Bohrmann, G. (2014, 11). Gas emissions at the continental margin west of Svalbard: mapping, sampling, and quantification. *Biogeosciences*, *11*(21), 6029–6046. doi: 10.5194/bg-11-6029-2014

Saunois, M., Martinez, A., Poulter, B., Zhang, Z., Raymond, P. A., Canadell, J. G., ... Zhuang, Q. (2024, 6). Global Methane Budget 2000-2020. *Earth System Science Data*. Retrieved from `https://doi.org/10.5194/essd-2024-115` doi: 10.5194/essd-2024-115

Seabrook, S., Thurber, A., Ladroit, Y., Discovery, K., Cummings, V., Tait, L., ... Hawes, I. (2023). Emergent Antarctic seaoor seeps: A tipping point reached?

doi: 10.21203/rs.3.rs-3657723/v1

Spain, E. A., Johnson, S. C., Hutton, B., Whittaker, J. M., Lucieer, V., Watson, S. J., … Coffin, M. F. (2020, 3). Shallow Seafloor Gas emissions Near Heard and McDonald Islands on the Kerguelen Plateau, Southern Indian Ocean. *Earth and Space Science*, *7*(3). doi: 10.1029/2019EA000695

Stein, A. F., Draxler, R. R., Rolph, G. D., Stunder, B. J. B., Cohen, M. D., & Ngan, F. (2015, 12). NOAA's HYSPLIT Atmospheric Transport and Dispersion Modeling System. *Bulletin of the American Meteorological Society*, *96*(12), 2059–2077. doi: 10.1175/BAMS-D-14-00110.1

Steinle, L., Graves, C. A., Treude, T., Ferré, B., Biastoch, A., Bussmann, I., … Niemann, H. (2015, 4). Water column methanotrophy controlled by a rapid oceanographic switch. *Nature Geoscience*, *8*(5), 378–382. doi: 10.1038/ngeo2420

Suaria, G., Perold, V., Lee, J. R., Lebouard, F., Aliani, S., & Ryan, P. G. (2020, 3). Floating macro- and microplastics around the Southern Ocean: Results from the Antarctic Circumnavigation Expedition. *Environment International*, *136*. doi: 10.1016/j.envint.2020.105494

Thoning, K. W., Tans, P. P., & Komhyr, W. D. (1989, 6). Atmospheric carbon dioxide at Mauna Loa Observatory: 2. Analysis of the NOAA GMCC data, 1974–1985. *Journal of Geophysical Research: Atmospheres*, *94*(D6), 8549–8565. doi: 10.1029/JD094iD06p08549

Thurber, A. R., Seabrook, S., & Welsh, R. M. (2020, 7). Riddles in the cold: Antarctic endemism and microbial succession impact methane cycling in the Southern Ocean. *Proceedings of the Royal Society B: Biological Sciences*, *287*(1931). doi: 10.1098/rspb.2020.1134

Tilbrook, B. D., & Karl, D. M. (1994). Dissolved methane distributions, sources, and sinks in the western Bransfield Strait, Antarctica. *Journal of Geophysical Research*, *99*(C8), 16383. doi: 10.1029/94jc01043

Veloso, M., Greinert, J., Mienert, J., & Batist, M. D. (2019, 2). Corrigendum: A new methodology for quantifying bubble flow rates in deep water using splitbeam echosounders: Examples from the Arctic offshore NW-Svalbard. *Limnology and Oceanography: Methods*, *17*(2), 177–178. doi: 10.1002/lom3.10313

Vogt, J., Risk, D., Bourlon, E., Azetsu-Scott, K., Edinger, E. N., & Sherwood, O. A. (2023, 5). Sea–air methane flux estimates derived from marine surface observations and instantaneous atmospheric measurements in the northern Labrador Sea and Baffin Bay. *Biogeosciences*, *20*(9), 1773–1787. doi: 10.5194/bg-20-1773-2023

Wallmann, K., Riedel, M., Hong, W. L., Patton, H., Hubbard, A., Pape, T., … Bohrmann, G. (2018, 12). Gas hydrate dissociation off Svalbard induced by isostatic rebound rather than global warming. *Nature Communications*, *9*(1). doi: 10.1038/s41467-017-02550-9

Wanninkhof, R. (2014, 6). Relationship between wind speed and gas exchange over the ocean revisited. *Limnology and Oceanography: Methods*, *12*(6), 351–362. doi: 10.4319/lom.2014.12.351

Weber, T., Wiseman, N. A., & Kock, A. (2019, 10). Global ocean methane emissions dominated by shallow coastal waters. *Nature Communications*, *10*(1). doi: 10.1038/s41467-019-12541-7

Westbrook, G. K., Thatcher, K. E., Rohling, E. J., Piotrowski, A. M., Pälike, H., Osborne, A. H., … Aquilina, A. (2009, 8). Escape of methane gas from the seabed along the West Spitsbergen continental margin. *Geophysical Research Letters*, *36*(15), n/a–n/a. doi: 10.1029/2009gl039191

Whiticar, M. J. (1999, 9). Carbon and hydrogen isotope systematics of bacterial formation and oxidation of methane. *Chemical Geology*, *161*(1-3), 291–314. doi: 10.1016/s0009-2541(99)00092-3

Wiesenburg, D. A., & Guinasso, N. L. (1979, 10). Equilibrium solubilities of methane, carbon monoxide, and hydrogen in water and sea water. *Journal of Chemical & Engineering Data*, *24*(4), 356–360. doi: 10.1021/je60083a006

Wilson, S. T., Bange, H. W., Arévalo-Martínez, D. L., Barnes, J., Borges, A. V., Brown, I., … Rehder, G. (2018, 10). An intercomparison of oceanic methane and nitrous oxide measurements. *Biogeosciences*, *15*(19), 5891–5907. doi: 10.5194/bg-15-5891-2018

Workman, E., Delille, B., Squires, F., Jones, A., Fisher, R., France, J., & Linse, K. (2024, 11). *Concentration of atmospheric methane and carbon dioxide and dissolved methane in surface water and water column in Scotia and Weddell Seas during the cruise DY158 in December 2022 and January 2023.* NERC EDS UK Polar Data Centr.

Workman, E., Dornan, T., & Saunders, R. (2024, 11). *Raw acoustic data collected by an EK80 echo sounder in Stromness Bay, South Georgia during the cruise DY158 on 5 January 2023.* NERC EDS UK Polar Data Centre.

Workman, E., Fisher, R. E., France, J. L., Linse, K., Yang, M., Bell, T., … Jones, A. E. (2024, 7). Methane Emissions From Seabed to Atmosphere in Polar Oceans Revealed by Direct Methane Flux Measurements. *Journal of Geophysical Research: Atmospheres*, *129*(14). doi: 10.1029/2023JD040632

Ye, W., Arévalo-Martínez, D. L., Li, Y., Wen, J., He, H., Zhang, J., … Zhan, L. (2023, 4). Significant methane undersaturation during austral summer in the Ross Sea (Southern Ocean). *Limnology and Oceanography Letters*, *8*(2), 305–312. doi: 10.1002/LOL2.10315

Yoshida, O., Inoue, H. Y., Watanabe, S., Suzuki, K., & Noriki, S. (2011). Dissolved methane distribution in the South Pacific and the Southern Ocean in austral summer. *Journal of Geophysical Research: Oceans*, *116*(7). doi: 10.1029/2009JC006089

Zhou, S., Meijers, A. J., Meredith, M. P., Abrahamsen, E. P., Holland, P. R., Silvano, A., … Østerhus, S. (2023, 7). Slowdown of Antarctic Bottom Water export driven by climatic wind and sea-ice changes. *Nature Climate Change*, *13*(7), 701–709. doi: 10.1038/s41558-023-01695-4

Zhu, R., Liu, Y., Ma, E., Sun, J., Xu, H., & Sun, L. (2009, 5). Greenhouse gas emissions from penguin guanos and ornithogenic soils in coastal Antarctica: Effects of freezing–thawing cycles. *Atmospheric Environment*, *43*(14), 2336–2347. doi: 10.1016/j.atmosenv.2009.01.027

Zhu, Y., Purdy, K. J., Martínez Rodríguez, A., & Trimmer, M. (2023, 6). A rationale for higher ratios of CH4 to CO2 production in warmer anoxic freshwater sediments and soils. *Limnology and Oceanography Letters*, *8*(3), 398–405. doi: 10.1002/lol2.10327